Pergamon

Bioorganic & Medicinal Chemistry 9 (2001) 1097–1113

BIOORGANIC & MEDICINAL CHEMISTRY

Inhibition of the HIV-1 Rev–RRE Complex Formation by Unfused Aromatic Cations

Ge Xiao, Arvind Kumar, Ke Li, C. Ted Rigl, Miroslav Bajic, Tina M. Davis, David W. Boykin* and W. David Wilson*

Department of Chemistry, Georgia State University, Atlanta, GA 30303, USA

Received 4 October 2000; accepted 21 November 2000

Abstract—RNA viruses cause a wide range of human diseases. Development of new agents to target such viruses is an active area of research. Towards this goal, a series of diphenylfuran cations as potential inhibitors of the Rev–RRE complex have been designed and synthesized. Analysis of the interaction of the diphenylfurans with RRE and TAR RNA model systems by gel shift assays indicates that they exhibit both sequence and structure-dependent binding modes. Our results show a strong interaction between the diphenylfuran ring system and RRE bases, while the TAR interactions are much weaker with the compounds that are the best inhibitors of Rev–RRE.

Introduction

Biological RNAs fold into locally base paired secondary regions and macromolecular tertiary structures that are essential for the biological functions of the RNA.[1–4] The DNA double helix is recognized primarily through its linear array of base pairs whereas proteins are recognized through their shape and three dimensional arrangement of functional groups. The single strands of most biological RNAs can assume folded structures that have features similar to both double-helical DNA as well as to the folded conformations of proteins. The highly-folded structures obtained from high-resolution structural investigations on RNA suggest that selected sites on such folded RNAs should be amenable to small-molecule drug-design strategies.[5–14] This approach would be similar to the highly successful application of such strategies to design compounds to target the active sites of proteins.

Recent high-resolution NMR studies with aminoglycoside–RNA complexes have defined the recognition principles for the antimicrobial activity of aminoglycosides.[2,15,16] Other studies have shown that aminoglycosides can inhibit RNA splicing,[17] ribozyme activity,[18–20] and can selectively inhibit both the Rev and Tat proteins from binding to their cognate RRE and TAR RNA binding sites in the genomic RNA of HIV-1.[21–23] Results from a range of experiments with other ribosome targeting antibiotics, such as thiostrepton, also indicate that RNA binds small molecules with high specificity and can be a highly specific therapeutic target.[24,25] These observations suggest that RNA is an underutilized therapeutic target and efforts are underway in several labs to design drugs that are selective for RNA–protein complexes.

The relative inhibitory effects of aminoglycosides against the formation of RRE–Rev complexes was determined by Zapp and co-workers[23] with a competitive gel shift assay that used an RRE IIB hairpin model system and a recombinant Rev protein. The relative activity of aminoglycosides to inhibit formation of the Rev–RRE complex was found to be: neomycin B (0.1 μM) > tobramycin (1.0 μM) > gentamicin (10 μM) > kanamycin A (≥100 μM) > streptomycin (≥100 μM), and these results suggest a structure-dependent recognition of the RRE RNA by neomycin and closely related aminoglycosides.[23] Although aminoglycosides are not ideal antivirals for reasons such as transport and toxicity, they do provide exciting new leads for development.

Efforts in our laboratory to design compounds that specifically recognize RNA and exert desired biological effects initially focused on identifying molecular structures that can recognize different RNA conformations.[14,26–28] Through this search an unfused aromatic diphenylfuran tetracation (DB182) that bound strongly to the RRE RNA of HIV-1 and inhibited complex formation with the Rev protein was found in a gel band shift assay similar to that described above for the aminoglycosides.[26,27]

*Corresponding authors. Tel.: +1-404-651-3798; fax: +1-404-651-1416; e-mail: chedwb@panther.gsu.ed (D.W. Boykin). Tel.: +1-404-651-3903; fax: +1-404-651-2751; e-mail: chewdw@panther.gsu.edu (W.D. Wilson)

0968-0896/01/$ - see front matter
PII: S0968-0896(00)00344-8

More detailed studies of the DB182–RRE complex suggested that the compound interacts strongly with the bases of RRE, requires the G–G and G–A base pair mismatches and internal loop region of RRE (Fig. 1(A)), and causes a conformational change in RRE on complex formation.[26]

The exciting findings on unfused aromatic cation–RNA interactions prompted us to initiate a range of synthetic and biophysical studies to obtain additional information on the interaction of unfused aromatic tetracations with RRE. A key goal of our efforts to design RNA selective drugs is to increase both the affinity and selectivity of the compounds for the RRE structure. In order to evaluate the importance of each structural component of DB182 to the inhibition of the Rev–RRE complex, a number of new derivatives in which the furan and phenyl groups and cationic substituents of the compound have been systematically varied have been prepared (Figs 2(b), 4(a) and (b), and 5(a)–(c)). Inhibition of Rev–RRE complex formation by the compounds has been evaluated through gel band shift experiments. The new diphenylfuran derivatives can be divided into four groups with modifications in the (1) cationic substituents, (2) phenyl rings, (3) central furan heterocycle, and (4) position of the cationic side chain (*meta* versus *para*) relative to the parent compound. One of the new compounds has six positive charges, several have two positive charges, and the majority have four positive charges. The objectives of the studies reported here are to determine how the components and structure of the diphenylfuran derivatives affect the activity and specificity for inhibition of the Rev–RRE complex, and in the long term, to use this information to design new compounds with enhanced RRE RNA interactions and inhibition selectivity for the Rev–RRE complex.

Results

Gel band shift analysis of the RRE duplex–Rev model system

To evaluate the ability of the compounds to inhibit the Rev–RRE complex, we have used the RRE duplex, defined by Gait and co-workers[29] and the Rev-17 peptide of Frankel and co-workers[30] in our assay for compound activity. The RRE hairpin defined by Peterson and co-workers[31] and Rev-17 peptide model system were also used here for some selected compounds for validation comparison. Complex formation between the Rev-17 peptide and RRE duplex model and hairpin (Fig. 1(A)) was evaluated with a gel band shift assay (Fig. 1(B)) as previously described.[32,33] Under the conditions used in these experiments, the RNA duplex and the hairpin shift from the free to the complex species over a sharp range of Rev peptide concentrations (Fig. 1). The RRE sample in the gel shift study migrates as an intact duplex or hairpin and forms a specific complex with Rev peptide. The interaction is quite specific and addition of the Tat peptide to the RRE RNA showed no complex formation over the same concentration range (not shown).

Aminoglycosides. In Figure 2(a); a competitive gel band shift assay illustrates the potential of aminoglycosides to inhibit the RRE duplex–Rev peptide complex under the experimental conditions of this work. IC_{50} values, the concentration of the compound required to give 50% inhibition of Rev binding to RRE, are given for each compound. As Zapp et al.[23] showed with an RRE–Rev model system, neomycin B demonstrates a strong inhibitory effect against the formation of the RRE duplex–Rev complex and was followed by tobramycin and gentamicin. Kanamycin A and streptomycin have no significant inhibitory effect under these conditions (Fig. 2(a)). With the duplex RNA model system and higher

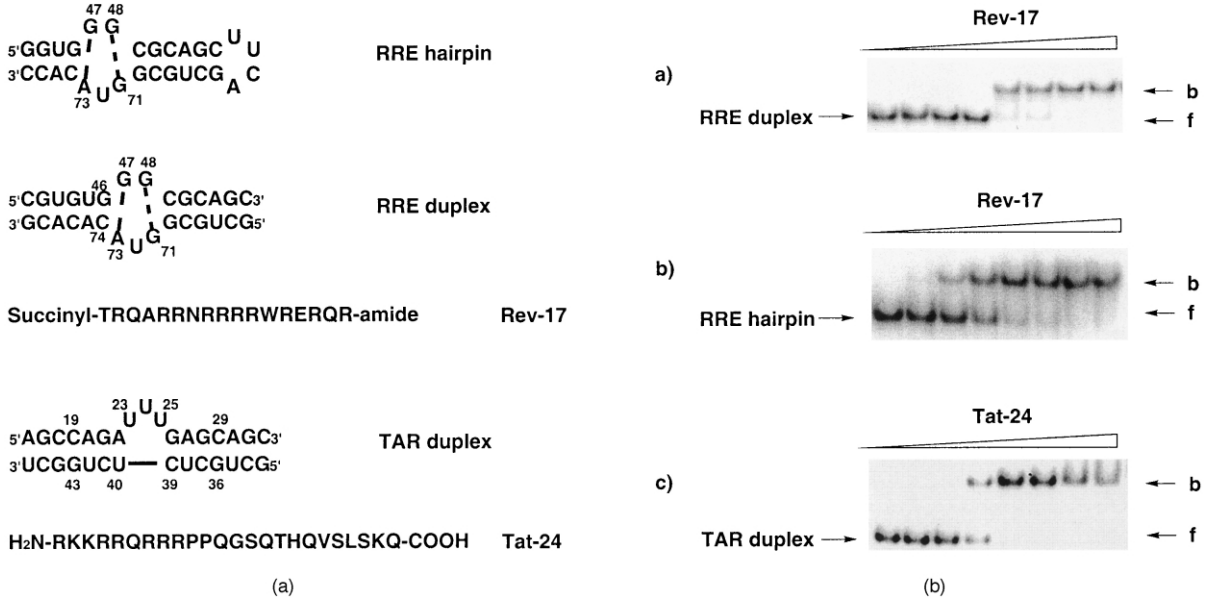

Figure 1. (A) RRE IIB duplex, hairpin, and TAR duplex models used in thermal denaturation experiments and gel shift assays. Sequences of the Rev-17 peptide from HIV-1 Rev protein and Tat-24 peptide from HIV-1 Tat protein that bind RRE and TAR RNAs, respectively, used in gel shift assays. (B) Gel shift assays of (a) RRE duplex titrated with Rev-17 peptide; (b) RRE hairpin titrated with Rev-17 peptide; (c) TAR duplex titrated with Tat-24 peptide.

temperature used for the gel band shift analysis in the present experiments, a higher concentration of neomycin is required to inhibit the Rev–RRE complex than in previous studies. The higher temperature is preferred for these experiments since we have observed significantly less smearing of RNA bands that occurs in the presence of increasing concentrations of some of the cationic compounds at low temperatures. T_m increases caused by addition of the aminoglycosides to the RRE duplex are also shown in Figure 2 for evaluation of the relative binding affinity of these compounds to the RRE RNA. The effect of the ratio of neomycin to RRE duplex on the observed *T*m is illustrated in Figure 3. Both the T_m increases and the ability to inhibit the Rev–RRE complex increase for the aminoglycosides as their charge increases (Fig. 2(a)).

Unfused aromatic cations. In our search for novel inhibitors of the RRE–Rev complex, it was previously shown that the diphenylfuran tetracation DB182 strongly inhibited binding of both the Rev protein and peptide model system to RRE.[26] Results for DB182 are shown in Figure 2(b) for reference under the gel conditions of this paper along with results for DB60, which was

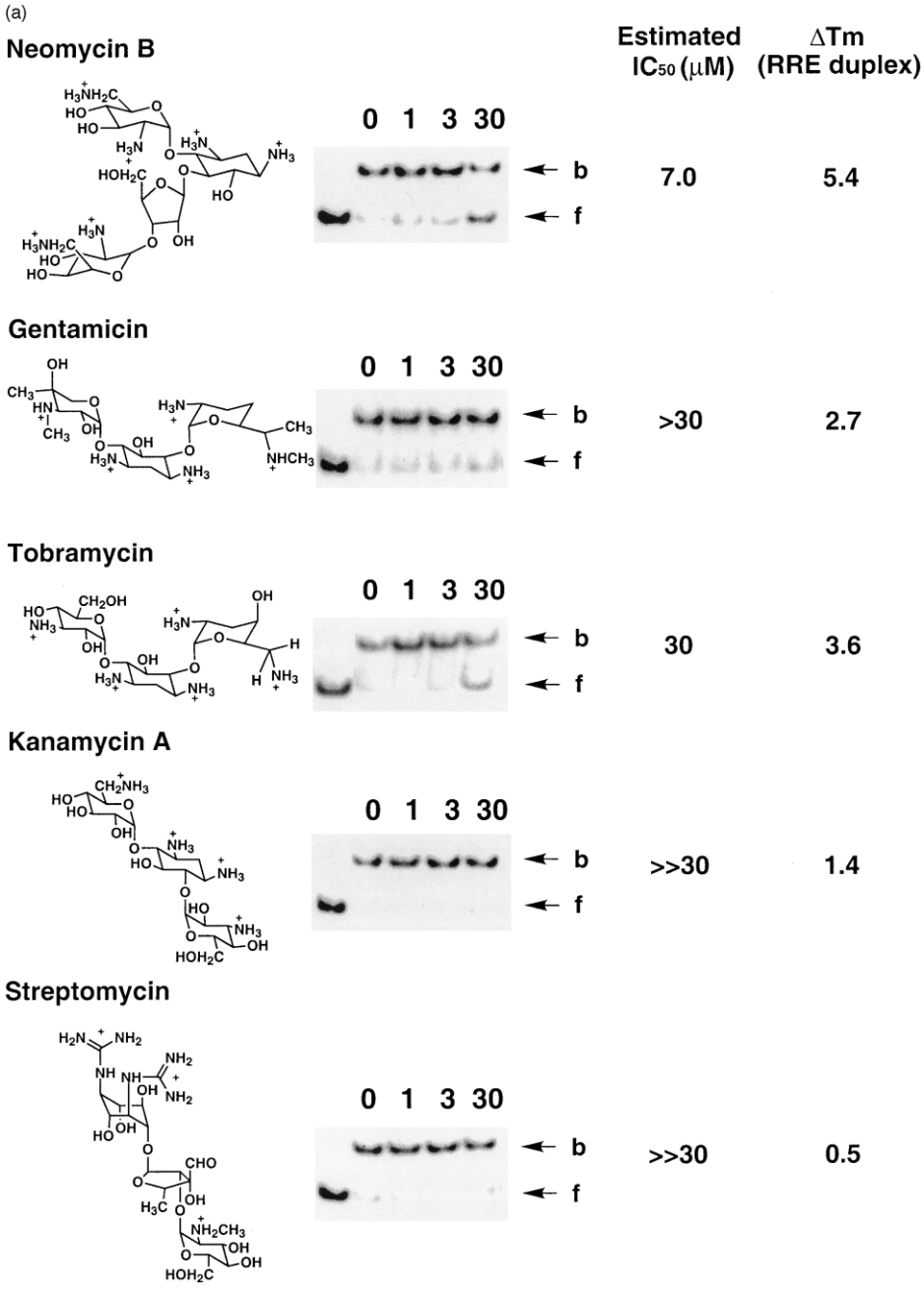

Figure 2. Competitive gel shift assays of the inhibition of the RRE–Rev interaction and IC_{50} values, the compound concentration required to give 50% bound RNA, and the increase in RRE T_m are shown. In each gel experiment, the first lane is RRE alone and subsequent lanes are RRE plus Rev-17 peptide and increasing concentration of drug (indicated in μM). The notations b and f indicate bound and free RRE, respectively. (a) RRE titrated with aminoglycosides; (b) RRE titrated with the diphenylfuran analogues that previously demonstrated inhibition of the Rev–RRE interaction.[26] (*continued on next page*)

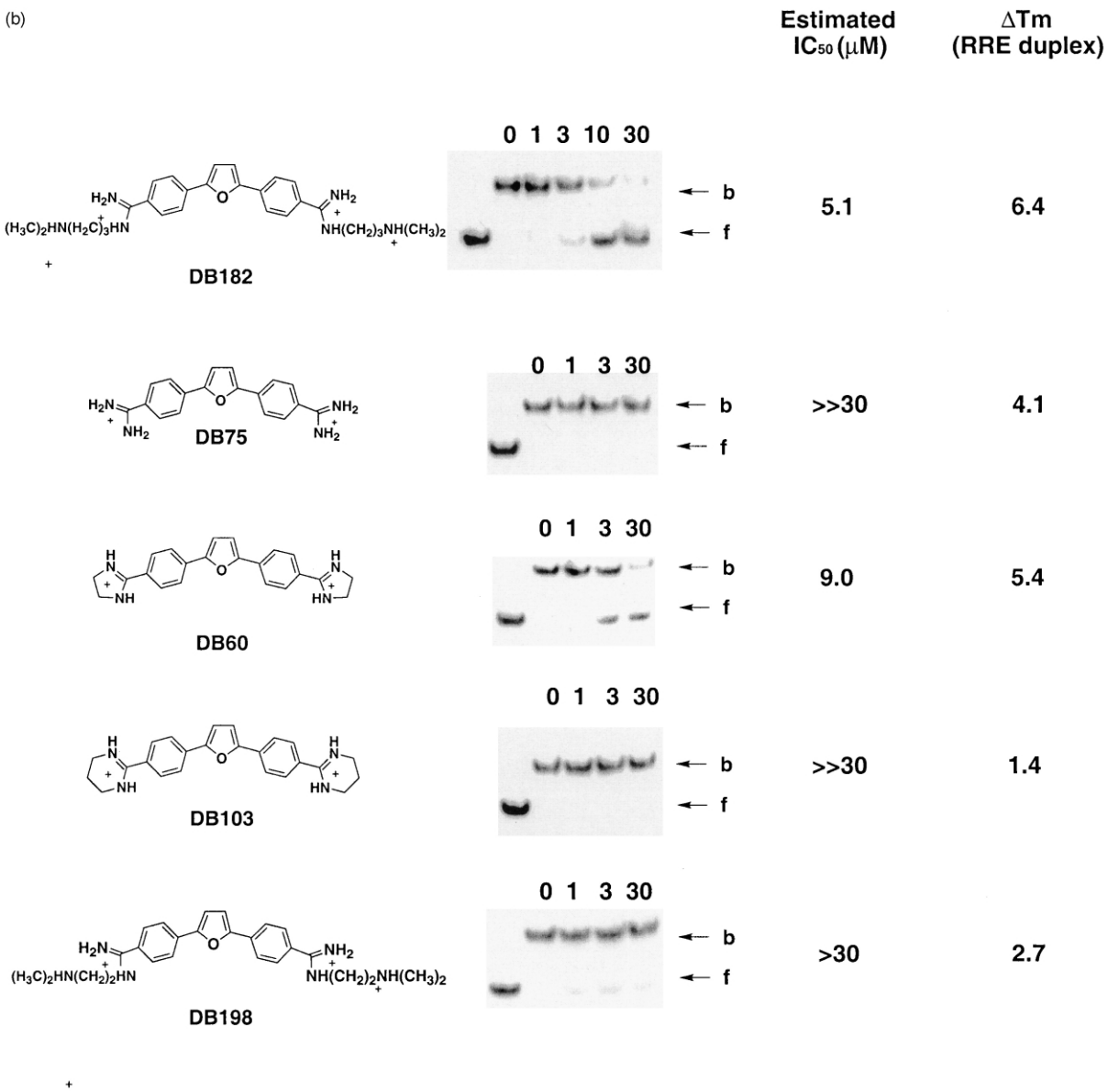

Figure 2. (*continued*)

previously found to be a significant but weaker inhibitor than DB182, and for DB75, DB103, and DB198, which were found to be very poor inhibitors. As can be seen, the agreement with previous work is excellent for all compounds, and DB182 is a significantly better inhibitor of the Rev–RRE interaction than neomycin.

The T_m increases for RRE caused by addition of the diphenylfuran derivatives are also shown in Fig. 2b for comparison with results for the aminoglycosides and with results for the new compounds reported here. Plots of the T_m increase versus ratio for several of the furan derivatives are compared to results for neomycin in Figure 3. The largest T_m increase occurs between the ratios of zero and one compound per duplex and there is little increase in T_m above a ratio of 2.

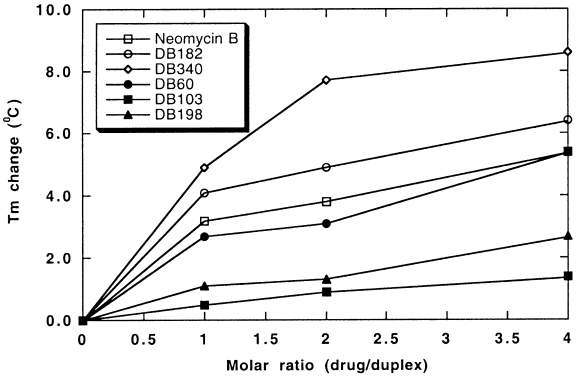

Figure 3. Melting temperature of the RRE–drug complex at varying ratios of drug to RRE.

To dissect the contributions that individual molecular units of DB182 make to the inhibition of Rev–RRE complex formation, four different series of new derivatives were designed, synthesized and are reported below. The compounds of Figure 4(a) have modified cationic substituents while those of Figure 4(b) have modified central furan heterocycles. The compounds of Figure 5(a) have modifications at one or both phenyl rings while the compounds of Figure 5(b) have the side chains moved from the *para* to the *meta* position.

Modification of the cationic substituents. As shown in Figure 4(a), compound DB339, in which the two amidine groups were changed to amide groups (a dication), showed only very slight inhibition at 30 μM, a significant decrease in activity compared to results for DB182 (Fig. 2(b)). DB240 and DB403, dications that retain the alkylamidine substituents with the removal of the terminal amino groups, also show no inhibition up to 30 μM. Compounds DB378 and DB379 with one or three more methylene groups in the cationic alkyl linker

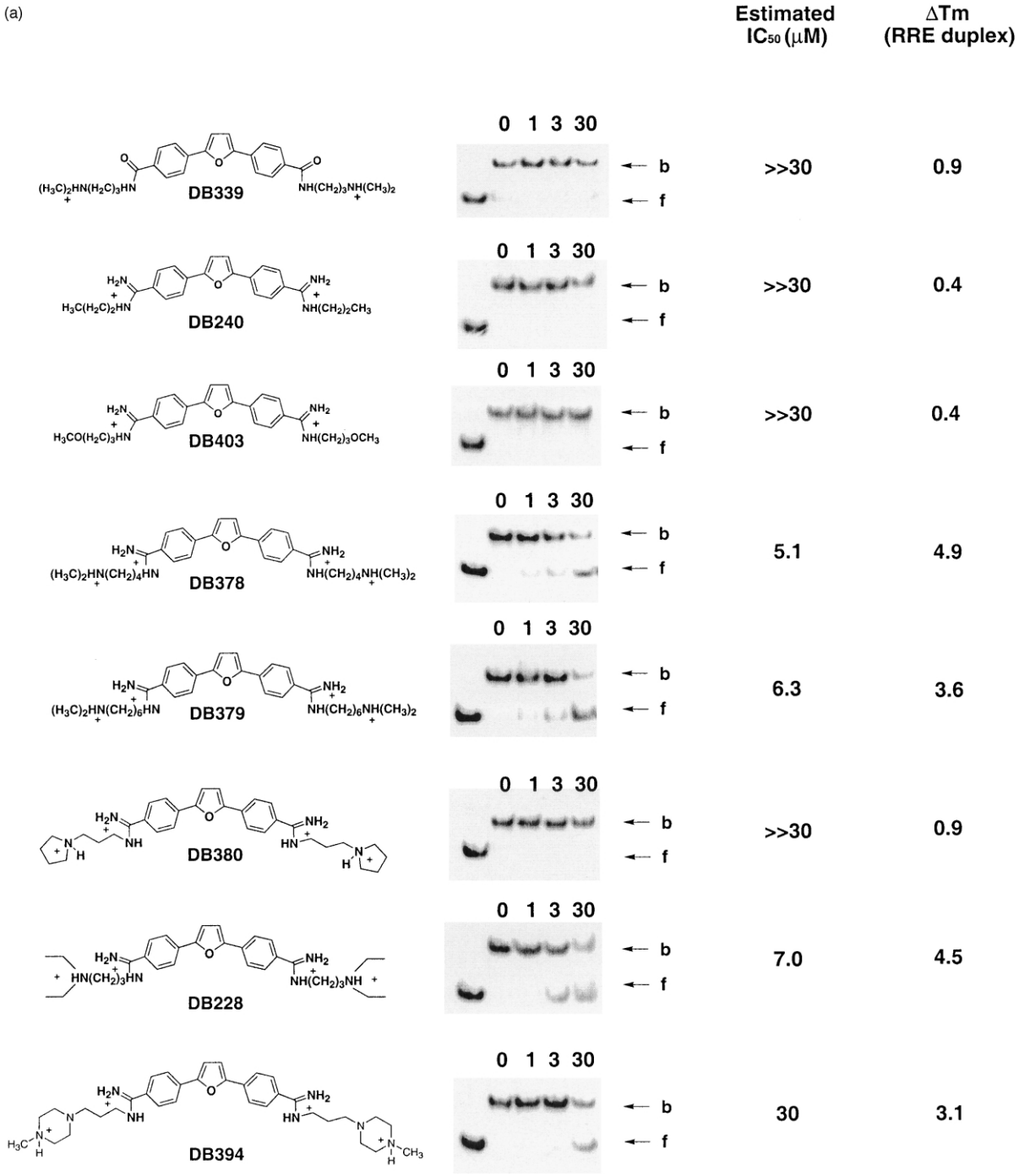

Figure 4. Competitive gel shift assays for inhibition of the RRE duplex–Rev interaction and the increase in RRE melting temperature by diphenylfuran analogues. Conditions and labels are the same as in Fig. 2. (a) Diphenylfuran analogues with modified cationic substituents; (b) diphenylfuran analogues with modified central furan heterocycles. (*continued on next page*)

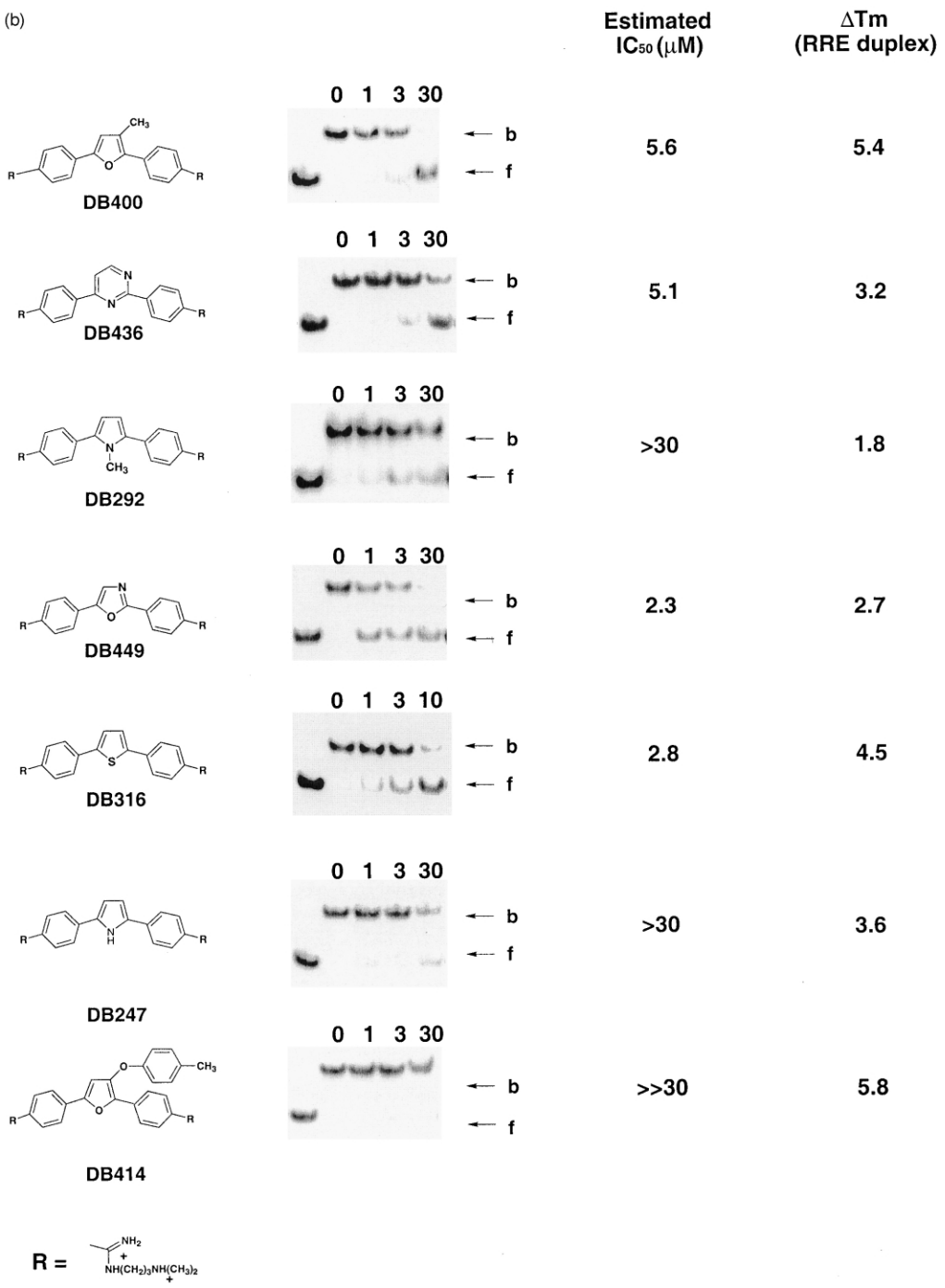

Figure 4. (*continued*)

than DB182, showed activity similar to DB182. When the terminal dimethylamino group of DB182 was replaced by a diethylamino group, DB228, the inhibitory activity decreased slightly. When the diethyl groups were fused into a five member ring, DB380, however, there was no inhibition of the Rev–RRE complex up to 30 μM. Similarly, DB394 with a terminal piperazyl ring is a very poor inhibitor. Clearly, inhibition of formation of the protein–RNA complex is acutely sensitive to the nature of the alkylamine substituent on the diphenylfuran aromatic system.

Compounds of Figure 4(a) that are very poor inhibitors have low ΔT_m values for their RRE complexes (less than 1 °C). The better inhibitors have ΔT_m values of 3–5 °C, but ΔT_m values in general are only qualitative predictors of IC_{50} results for Rev–RRE inhibition.

Modification or removal of the central furan heterocycle. Compound DB400, in which the 3-position of furan is substituted with a methyl group has similar activity to the parent compound DB182, while a compound with a 3-tolyloxy substituent, DB414, is inactive (Fig. 4(b)). In

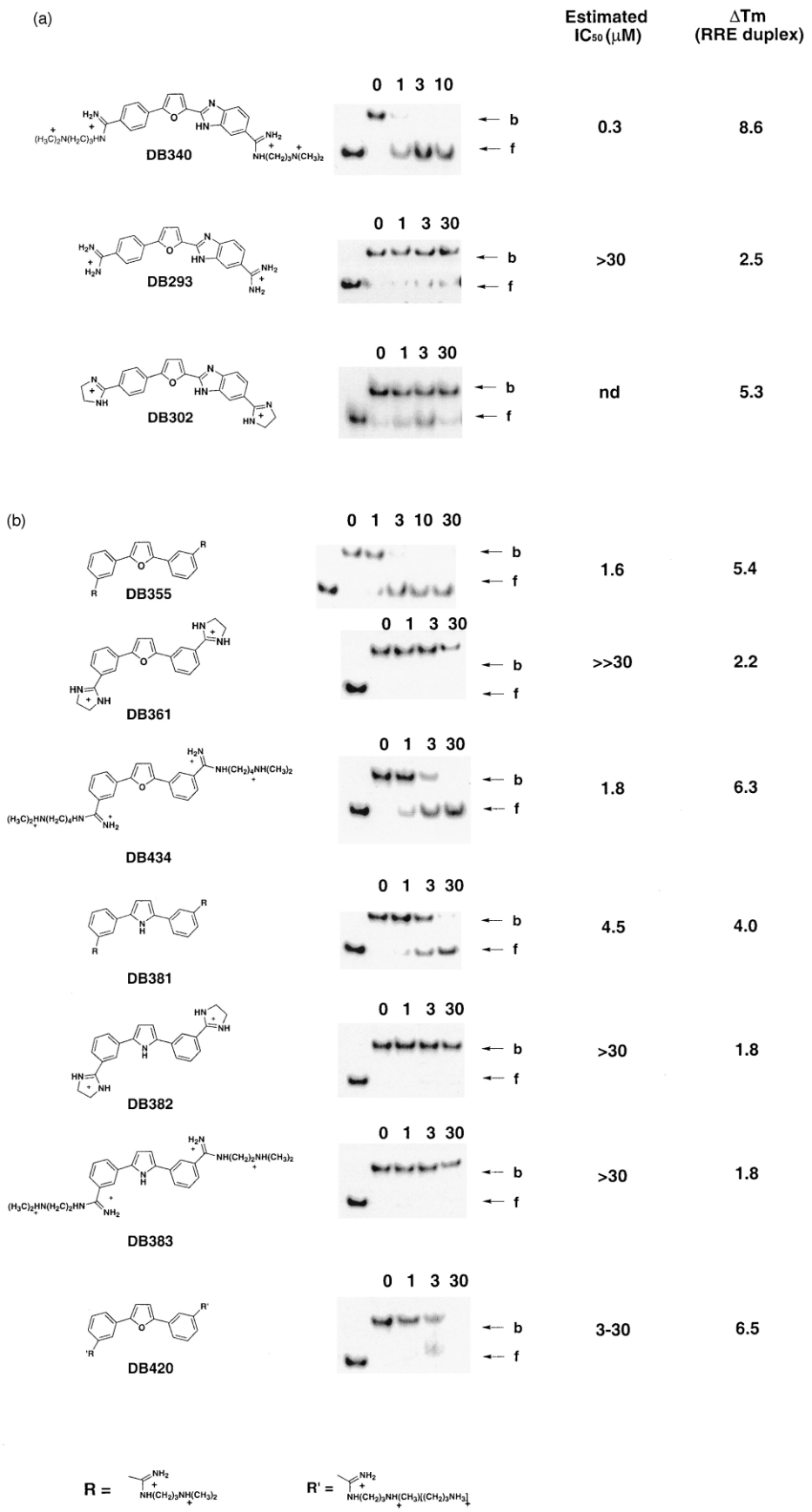

Figure 5. Competitive gel shift assays for inhibition of the RRE–Rev interaction and the increase in RRE melting temperature by diphenyfuran analogues. Conditions and labels are the same as in Fig. 2. (a) Inhibition of the RRE duplex–Rev interaction by diphenylfuran analogues with modified phenyl rings; (b) inhibition of the RRE duplex–Rev interaction by diphenylfuran analogues with the position of the cationic substituent modified; (c) inhibition of the RRE hairpin–Rev interaction by selected diphenylfuran analogues. (*continued on next page*)

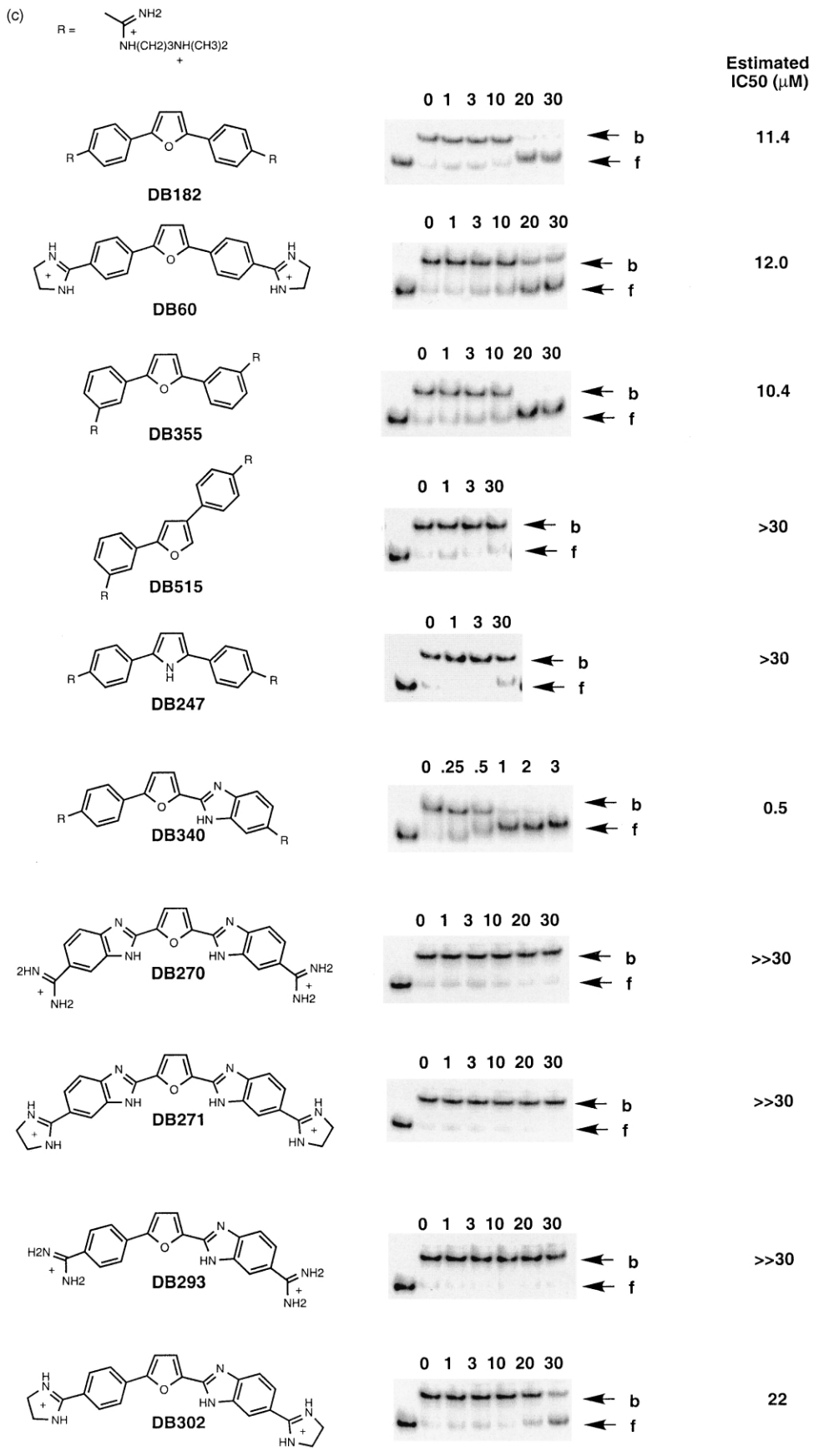

Figure 5. (*continued*)

agreement with previous results,[27] the corresponding pyrrole compound, DB247, showed significantly decreased activity with an IC_{50} greater than 30 μM. Relative to the furan DB182, the corresponding thiophene, DB316, and oxazole, DB449, compounds have improved activity and the pyrimidine, DB436, has similar activity. The oxazole compound DB449 was the most active compound in the series of derivatives in Figure 4, and it is clear that the central heterocyclic ring has a strong influence on the inhibitory activity. Several carbocyclic tetracations that are closely related to DB182 are completely inactive in the assay (not shown).

As observed with the compounds of Figure 4(a), there is a general correlation between ΔT_m and inhibition, but the correlation is not quantitative. T_m increases for the RRE RNA complex with these compounds are generally larger for the better inhibitors than for the poor inhibitors, suggesting that binding strength for the RRE RNA is a primary factor in effectiveness of the compounds as Rev–RRE inhibitors. Although all active compounds have significant ΔT_m values, some inactive compounds have ΔT_m values close to the values for the active compounds. These results can be explained by the difference between specific and nonspecific binding. The T_m increase is determined by the increased stability of the entire RNA and is sensitive to both specific and nonspecific binding while inhibition is much more dependent on specific interactions that prevent binding of the Rev peptide. Thus compounds such as DB379 and DB394 have very similar ΔT_ms but quite different IC_{50} values.

Modification of the phenyl rings. The compounds shown in Figure 5(a) have one or more of the phenyl rings of the DB182 diphenylfuran system replaced by a benzimidazole ring. The conversion of DB182 to DB340 has a dramatic effect and produced the most potent compound of the series with strong inhibition of Rev–RRE complex formation at an IC_{50} of less than 1 μM. The benzimidazole DB340 binds strongly to RRE and causes a large increase in the T_m of RRE on complex formation. Like the amidine dication analogue of DB182 (DB75 in Fig. 2(b)), the amidine dication analogue of DB340, DB293, is inactive. The imidazoline dication analogue of DB340, DB302, is less active than the imidazoline dication analogue of DB182 (DB60 in Fig. 2(a)). DB302 reproducibly gave some inhibition at 3 μM but less at 30 μM as in Figure 5(a). This may be due to a cooperative self-association of DB302 at the higher concentrations that limits its specific binding to RRE.

The position of the cationic substituent on the unfused aromatic ring system also has a strong effect on Rev–RRE inhibition. Compound DB355 (Fig. 5(b)), in which the *para* cationic substituents of DB182 are moved to the *meta* position, has a significantly improved activity (IC_{50} = 1.6 μM) relative to DB182 (IC_{50} of 5 μM). Interestingly, however, when the imidazole side chains of the dication DB60 (Fig. 2(b)) are moved to the *meta* position, DB361, a dramatic decrease in inhibition is observed, and there is no activity up to 30 μM. As with the *para* derivatives, addition of another methylene group to the side chain in the *meta* series, DB434, did not greatly affect inhibition while a derivative with a longer side chain and six total charges, DB420, resulted in an inactive compound. Although pyrroles DB382 and DB383 are inactive, the pyrrole analogue of DB182 has higher activity when the cationic substituents are *meta*, DB381, instead of *para*, DB247 (Fig. 2(b)), as observed with the corresponding *meta* and *para* furans. The conclusion from these results is that for compounds with a central five-membered ring heterocycle substituted at the 2- and 5-positions with phenyl groups, derivatives with meta cationic substituents are much better Rev–RRE inhibitors than the corresponding *para* substituents. As with the compounds described above, there is a general correlation of ΔT_m and inhibition ability for the compounds of Figure 5.

Gel band shift analysis of the RRE hairpin–Rev model system

In order to test the reliability of the RRE duplex model system, an RRE hairpin model system was used in the competitive gel shift assays. The conditions used are described in Experimental. Ten representative compounds were initially assayed (Fig. 5(c)) for their ability to inhibit Rev binding. From these results we can see that several of these aromatic heterocyclic compounds have significant inhibitory potential. In particular, the tetracationic compound DB340 was a potent inhibitor of Rev binding with an IC_{50} of 0.5 μM in the hairpin model that is within experimental error of the 0.3 μM value observed in the duplex model system. For the other compounds, the measured IC_{50} in the hairpin model system were generally somewhat larger than the corresponding results in the duplex model system. The order of the relative activity of these compounds in both of the model systems is the same, however: DB340 > > DB355 > DB182 > DB60 > DB247 > DB515. Four additional dicationic derivatives of DB340 (DB270, DB271, DB293, and DB302) were also assayed on this system (Fig. 5(c)). Among them, DB302 has the best inhibitory activity with IC_{50} of 22 μM. The others were not active up to 30 μM.

Inhibition specificity

In order to investigate the specificity of the inhibition of the Rev–RRE complex by the unfused aromatic tetracations, effects of representative compounds on a Tat peptide–TAR RNA duplex (Fig. 1(a)) were investigated (Fig. 6). The Tat-24 peptide used in this work is the same one characterized by Long and Crothers[34] while the TAR duplex (Fig. 1(a)) was shown to form a high affinity site for the Tat protein by Gait and co-workers.[29] The titration of labeled TAR RNA by the peptide is shown in Figure 1(b), and, as with the RRE titration by Rev, complex formation occurs over a narrow concentration range. Compound DB182 inhibits the Tat–TAR complex with IC_{50} of 3.6 μM. Pyrrole DB247, a poor inhibitor in the Rev–RRE system, has improved activity against Tat–TAR. Compounds DB340 and DB355, the most active in the Rev–RRE assay, show significantly reduced activity against the Tat–TAR complex with IC_{50} values greater than 15 μM. The conclusion from these results is that the most active compounds of this series in the

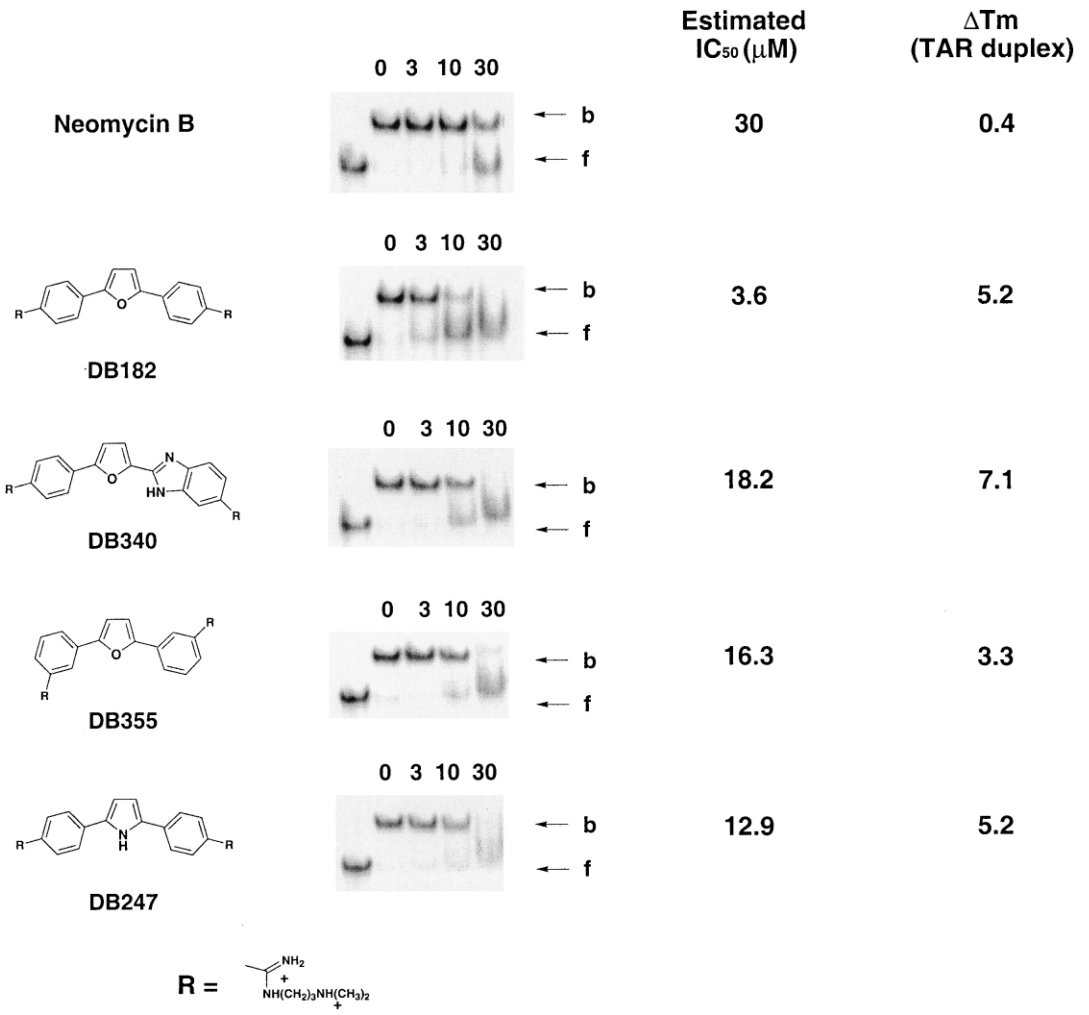

Figure 6. Competitive gel shift assays for inhibition of TAR–Tat interaction and the increase in TAR melting temperature by neomycin B and representative diphenylfuran analogues. The first lane is TAR alone and subsequent lanes are TAR plus Tat-24 and increasing concentration of drug (indicated in μM). The notations b and f indicate bound and free TAR, respectively.

Rev–RRE assay are also the compounds which have the most significant specificity for the Rev–RRE system. No correlation of ΔT_m and the ability to inhibit the Tat–TAR complex is apparent with these compounds.

Discussion

The RRE duplex RNA system used in the assays reported here provides a convenient synthetic model system that is readily amenable to modification of the base sequence or backbone chemistry on each strand.[29,33] The duplex forms a specific complex with the Rev-17 peptide (Fig. 1(a) and (b)) while addition of the Tat peptide does not yield a complex under the same conditions (not shown). Similar results are obtained with inhibition of Rev binding with the RRE hairpin. The RRE–Rev complex and free RRE are resolved in nondenaturing gel electrophoresis experiments (Fig. 1(B)), and this provides a method for analysis of inhibition of complex formation by added agents. Control experiments with aminoglycosides and the duplex–peptide model system (Fig. 2(a)) are in agreement with previous studies with the Rev protein and RRE hairpin model system.[23,26,27] Significant inhibition of complex formation is obtained with neomycin while other related aminoglycosides have reduced inhibition ability.

Our previous results for the compounds in Fig. 2(b) with the Rev protein and RRE hairpin complex indicated that DB182 is a strong inhibitor of complex formation, the dication DB60 is a moderate inhibitor while DB75, DB103 and DB198 are all poor inhibitors.[26,27] The results in Figure 2(b) with the duplex–peptide model are in good agreement with the previous results. For design of the compounds reported in this paper, we have treated DB182 as a lead compound that is composed of three components that should be modified in a structure–inhibition assay: a central heterocycle, phenyl rings that are symmetrically substituted on the heterocycle, and cationic substituents at the *para* positions of the phenyl rings. In the work reported here, we have individually varied each component as well as the position of the cationic substituent to determine how each molecular unit contributes to the observed Rev–RRE inhibition. The modifications have resulted in new compounds with significantly improved inhibitory activity.

Conversion of the two dicationic substituents into monocationic groups of similar structure yielded completely inactive compounds (Fig. 4(a)). Maintaining the charge while lengthening the alkyl chain between the amidine and amine or modifying the terminal amine either did not improve the activity or yielded completely inactive compounds. The IC_{50} values of Figure 4(a) show that inhibition of complex formation by the furan derivatives is quite sensitive to change in both the amidine and amine cations. It appears that two dicationic groups are required for specific binding and are critical for effective inhibition of the Rev–RRE complex. A small substitutent on the furan ring does not significantly change inhibition while a large substituent abolishes activity (Fig. 4(b)). The RNA interactions necessary for Rev inhibition are not available when the furan has a bulky substituent at the 3-position. It should be noted that the bulky *O*-toluyl substituent is twisted out of the diphenylfuran aromatic plane and could cause a significant perturbation in RNA interactions of the system.

The oxazole, thiophene and the six-membered pyrimidine heterocyclic compounds all have activity that is similar or slightly better than the parent furan (Fig. 4(b)). With a central five-atom ring, the oxazole and the thiophene derivatives are good inhibitors while the pyrrole is a very poor inhibitor (Fig. 4(b)). It appears that the RNA target site can accommodate either a central five or six-membered ring system, but the ring must have an H-bond accepting heteroatom at the 1-position. The pyrrole can bind to RRE and raise the global T_m value of the RNA, but although it has the correct shape, it apparently does not provide the correct type of interaction for binding strongly at the specific site required for Rev inhibition. IC_{50} values for DB340 and DB182 obtained through a solid-phase assay[35] agree with the IC_{50} values reported here obtained through gel shift assays. The IC_{50} value for the pyrrole DB247 obtained through the solid-phase assay is much lower than the value reported here. The reason for this discrepancy is currently unknown. It appears that IC_{50} values for strong binders such as DB340 and DB182 are in much better agreement than IC_{50} values for weak binders such as DB247.

When the cationic substituents are moved from the *para* to the *meta* positions, the furan derivative IC_{50} values decrease considerably (compare isomeric derivatives in Figs 4(b) and 5(b)). The pyrrole *meta* derivative also has some activity in contrast to the inactive *para* compound. Clearly the heterocycle requirement is relaxed in moving from the *para* to the *meta* substituted compounds. The *meta* imidazoline dication, however, completely loses activity (compare DB361 in Fig. 5(b) to DB60 in Fig. 2(b)) in the *para* to *meta* switch. All *meta* tetracations evaluated are more active that the corresponding *para* compounds, and equally as important, the *meta* furan derivative DB355 appears to be more specific for the Rev–RRE complex that the *para* derivative. The *para* compound actually has a slightly lower IC_{50} for the Tat–TAR complex than for the Rev–RRE system (compare DB182 in Figs 2(b) and 6) while the *meta* compound has a considerably lower IC_{50} for the Rev–RRE complex (compare DB355 in Figs 5(b) and 6).

The best inhibitor of all compounds in this series is the benzimidazole DB340 (Fig. 5(a)) which inhibits the complex at less than 1 μM concentration even under the relatively stringent conditions of the assay used in this study (e.g., relative to a 7 μM IC_{50} for neomycin).

The dicationic analogues of DB340 show poor activity and the imidazoline derivative is less active than the dication diphenylfuran compounds DB60 and DB75 (Fig. 2(a)). The imidazoline compound, DB302, is the only one in the series to show less activity at 30 μM than at 3 μM concentration and some secondary interactions may limit its specific binding to RRE duplex.

The most active compounds with the greatest specificity in this series are DB340 and DB355. The benzimidazole tetracation is also the most specific compound for the Rev–RRE system in this series with a ratio of Rev–RRE IC_{50} to that for the Tat–TAR complex greater than 50. If the reasonable assumption is made that DB340 and DB355 recognize RRE through a similar conformation, it becomes useful to establish conformational similarities between these two compounds as well as how they differ from derivatives with lower activity. One obvious difference between the highly active DB340 and DB355 relative to the parent *para* compound DB182 is that with DB182, rotation about the phenyl–furan bond does not yield a new conformation while in the *meta* compound it does. With the benzimidazole derivative DB340, rotating about the phenyl–furan bond does not yield a new conformation but rotation about the benzimidazole–furan bond does generate a new conformational state. It thus seems possible that asymmetric comformations of the active compounds account for the higher activity, perhaps conformations with the two cationic groups pointed in approximately opposite directions with respect to the aromatic ring system. Experiments are in progress to test this hypothesis.

The results presented here demonstrate that formation of the drug–RRE complex leading to inhibition of Rev binding is quite sensitive to the structure of the compound. A general model for inhibition of Rev–RRE complex formation has not yet been defined. However, footprinting and preliminary NMR results on the DB340–RRE complex suggest that DB340 binds near the internal loop region of RRE and competes with binding of the Rev peptide. Detailed binding experiments for other strong binders such as DB60, DB288, and DB355 should yield additional insight into the mechanism of Rev inhibition and aid in the identifying specific molecular motifs with high affinity for RNA.

Experimental

Compound synthesis. The compounds used in these experiments are shown in Figures 2, 4, and 5. All aminoglycosides were purchased from Sigma Chemical Company. The synthesis of compounds DB75, DB228, DB60, DB103, DB182, DB198, and DB240, DB403 have been published previously[26] and synthesis of all new com-

pounds are given below. The compounds were made into stock solutions with DEPC treated, autoclaved deionized water. Melting points were recorded using a Thomas Hoover (Uni-Melt) capillary melting point apparatus or a Fisher-Johns apparatus and are uncorrected. ^{1}H NMR and ^{13}C NMR spectra were recorded employing a Varian GX400 spectrometer and chemical shifts (δ) are in ppm relative to trimethylsilane (TMS) and coupling constants (*J*) are reported in Hertz. Mass spectra were recorded on a VG Instruments 70-SE spectrometer (Georgia Institute of Technology, Atlanta, GA). IR spectra were recorded using a Michelson 100 (Bomem, Inc.) instrument. Elemental analysis were obtained from Atlantic Microlab Inc. (Norcross, GA) and are within ± 0.4 of the theoretical values. All chemicals and solvents were purchased from Aldrich Chemical Co. or Fisher Scientific.

2-[5-(2-Imidazolinyl)-2-benzimidazolyl]-5-[4-(2-imidazolinyl) phenyl] furan hydrochloride DB302. A suspension of 2-(5-cyano-2-benzimidazolyl)-5-(4-cyanophenyl)furan (**31**) (0.5 g, 1.5 mmol) in 50 mL of absolute ethanol was cooled to 0–5 °C and was saturated with HCl (g). The flask was stoppered and contents was stirred at room temperature until IR spectra indicated the disappearance of the nitrile peak (ca. 5 days). Anhydrous ether was added to the suspension and solid was collected by filtration and washed with dry ether. The resultant di-imidate ester was suspended in absolute ethanol (50 mL) and ethylenediamine (0.23 g, 3.8 mmol) was added. The mixture was heated at reflux for 24 h and after cooling ether was added. The solid was collected by filtration and dried in vacuum at 90 °C for 48 h. The free base was suspended in absolute ethanol saturated with HCl and heated at reflux for 2 h. After cooling, dry ether was added and solid collected by filtration, washed with acetone and dry ether, and dried in vacuum at 90 °C for 48 h. Yield 0.58 g (75%) of yellow solid, mp > 290 °C. MS (FAB): *m*/*z* 397 ($M^+ + 1$); HRMS: calcd mass (free base): 397.1777 ($M^+ + 1$); observed mass: 397.1813. ^{1}H NMR (DMSO-d_6/D_2O, TMS): 8.28 (s, 1H), 8.17 (d, 2H, *J* = 8.4), 8.05 (d, 2H, *J* = 8.2), 7.85 (d, 1H, *J* = 8.2) 7.81(d, 1H, *J* = 8.8), 7.52 (d, 1H, *J* = 3.8), 7.47 (d, 1H, *J* = 3.8), 4.05 (s, 4H), 4.02(s, 4H). ^{13}C NMR (D_2O/DMSO-d_6): 165.6; 165.2; 155.2; 145.1; 142.4; 140.4; 137.1; 134.5; 129.7; 125.7; 125.6; 124.5; 121.3; 118.5; 117.2; 116.5; 113.1; 45.8. Anal. calcd for: $C_{23}H_{20}N_6O$•3HCl: C, 54.61; H, 4.58; N, 16.62; Cl, 21.03. Found: C, 54.67; H, 4.65; N, 16.63; Cl, 20.93.

2,5-Bis-4-*N*-(3-dimethylaminopropyl)amidinophenylthiophene DB316. A solution of freshly distilled 3-dimethylaminopropylamine (0.37 g, 3.6 mmol) in 2 mL absolute ethanol was added to a suspension of bis-imidate ester dihydrochloride (0.78 g, 1.7 mmol), prepared from 2,5-bis[4-cyanophenyl]thiophene,[36] in 30 mL ethanol (under nitrogen). The mixture was stirred at room temperature for 12 h and the excess solvent was distilled. The residue was washed with dry ether and dissolved in water, filtered and basified, while cooling and stirring, to yield a gummy mass. The solid was separated from the aqueous phase and dissolved in 60 mL of chloroform, dried over anhydrous Na_2SO_4, filtered and concentrated. The residue was triturated with cold dry ether and filtered to yield 0.51 g (77%) pale yellow solid, mp 168–170 °C dec. ^{1}H NMR (DMSO-d_6/45 °C) 7.77 (d, 4H, *J* = 8.4), 7.67 (d, 4H, *J* = 8.4), 7.54 (s, 2H), 3.18 (t, 4H, *J* = 6.8), 2.33 (t, 4H, *J* = 6.8), 2.16 (s, 12H), 1.12 (q, 4H, *J* = 6.8). M *m*/*e* 490 (M^+). An ethanolic solution of free base (0.3 g, 0.8 mmol) was saturated with dry HCl gas, stirred at room temperature for 3 h, the excess ethanol was removed under reduced pressure and the gummy yellow mass was triturated with dry ether, the solvent was removed under reduced pressure and the residue dried in vacuum at 50 °C for 12 h, yellow solid 0.41 g (80%); mp 294–296 °C dec. ^{1}H NMR (DMSO-d_6/D_2O/TSP) 7.87 (d, 4H, *J* = 8.4), 7.82 (d, 4H, *J* = 8.4), 7.70 (s, 2H), 3.53 (t, 4H, *J* = 7.2), 3.11 (t, 4H, *J* = 7.2), 2.73 (s, 12H), 2.07 (q, 4H, *J* = 7.2). ^{13}C NMR (DMSO-d_6/D_2O.TSP/45 °C) 163.1, 142.9, 138.2, 129.5, 127.8, 127.6, 125.9, 54.8, 42.9, 40.3, 23.0. Anal. calcd for: $C_{28}H_{38}N_6S$•4HCl•0.5H_2O C, 52.09; H, 6.71; N, 13.02. Found: C, 52.08; H, 6.73; N, 12.92.

2,5-Bis[4-{3-(*N*,*N*-dimethylaminopropyl)carbamoyl}phenyl] furan DB339. To a suspension of 2,5-bis[4-carboxyphenyl]furan diacid chloride (30) (0.69 g, 2 mmol) in 75 mL dry CH_2Cl_2 was added 3-(*N*,*N*-dimethylamino)propylamine (2 mmol) and the mixture was stirred at room temperature for 6 h. The solvent was removed by distillation and the solid residue was treated with ice-water, the pH was adjusted to 10 with 2 M NaOH and the solid which resulted was filtered, washed with cold water and crystallized from ether: $CHCl_3$ to yield a pale yellow solid (75% yield) mp 189–190 °C. The free base was converted to its HCl salt by treating with saturated ethanolic-HCl in an 85% yield of yellow hygroscopic solid mp 205–208 °C dec. ^{1}H NMR (DMSO-d_6) 10.91 (b, s, 2H), 8.80 (b, s, 2H), 8.03 (d, 4H, *J* = 8.4), 7.92 (d, 4H, *J* = 8.4), 7.23 (s, 2H), 3.40 (q, 4H, *J* = 6), 3.15 (quintet, 4H, *J* = 5.2), 2.76 (s, 6H), 2.75 (s, 6H), 2.02 (quintet, 4H, *J* = 6.8). ^{13}C NMR (DMSO-d_6/D_2O) 165.6, 152.4, 132.8, 131.9, 127.7, 122.9, 109.6, 54.3, 41.7, 36.2, 23.8 MS *m*/*e* 476 (M^+). Anal. calcd for: $C_{28}H_{36}N_4O_3$•2HCl•0.5H_2O C, 60.21; H, 7.03; N, 10.03. Found: C, 60.51; H, 7.13; N, 9.95.

2-{4-[*N*-(3-*N*,*N*-Dimethyaminopropyl)amidino]-2-benzimidazolyl}-5-[4-(3-*N*,*N*-dimethyaminopropyl)amidino]phenyl] furan-pentahydrochloride DB340. 2-(5-cyano-2-benzimidazolyl)-5-(4-cyanophenyl)furan (31) was converted into its imidate ester, subsequently allowed to react with 3-*N*,*N*-dimethyaminopropylamine, and finally converted into the hydrochloride salt using the procedure above for DB302 to yield a yellow solid (88% yield); mp 198–200 °C dec. ^{1}H NMR (DMSO-d_6/D_2O) 8.13 (d, 2H, *J* = 8), 8.09 (s, 1H), 7.89 (d, 2H, *J* = 8), 7.79 (d, 1H, *J* = 8.4), 7.64 (d, 1H, *J* = 8.4), 7.51 (d, 1H, *J* = 2.8), 7.43 (d, 1H, J = 2.8), 3.58–3.45 (m, 4H), 3.22–3.15 (m, 4H), 2.79 (s, 12H), 2.18–2.12 (m, 4H). ^{13}C NMR (DMSO-d_6/D_2O) 163.1, 162.0, 153.7, 144.6, 143.9, 142.2, 137.3, 133.1, 128.9, 127.7, 123.9, 123.0, 122.8, 115.8, 115.4, 114.3, 110.7, 53.8, 41.8, 40.1, 22.3, 22.3. MS *m*/*e* 515 (M^+). Anal. calcd for: $C_{29}H_{38}N_8OHCl$•2.5H_2O C, 46.89; H, 6.52; N, 15.10. Found: C, 46.82; H, 6.77; N, 15.35.

2,5-Bis[3-(2-imidazolinyl)phenyl]furan dihydrochloride DB361. Divinyl sulfone (5.9 g, 5 mmol) in 20 mL dry ethanol was added to a boiling mixture of *m*-bromobenzaldehyde (18.5 g, 1 mmol), anhydrous sodium acetate (2.46 g, 0.03 mol) and 3-benzyl-5(2-hydroxyethyl)thiazolium chloride (2.69 g, 0.01 mol) in 120 mL dry ethanol. The mixture was allowed to reflux for 16 h, cooled, filtered, washed with ether, water and dried. The solid was extracted with boiling chloroform (4×200 mL), the combined extracts were washed with a $NaHCO_3$ solution (20%) and dried over anhydrous sodium sulfate. The solution was passed through a silica gel column to yield after removing solvent a white crystalline solid 7.90 g (40%) mp 170–172 °C dec. ^{1}H NMR (DMSO-d_6) 8.09 (m, 2H), 7.89 (m, 2H), 7.82 (m, 2H), 7.5 (m, 2H), 3.39 (s, 4H). ^{13}C NMR (DMSO-d_6) 197.1, 138.4, 135.2, 130.4, 129.9, 126.4, 121.7, 32.3. MS *m*/*e* 396 (M^+). The 1,4-di(3-bromophenyl)butanedione thus obtained was used directly, without further characterization, in the next step.

To a solution of 1,4-di(3-bromophenyl)butanedione (7.92 g, 0.02 mol) in 80 mL boiling acetic anhydride, five drops of concd H_2SO_4 was added and the mixture was allowed to reflux for 5 min. The solution was cooled, poured on ice-water, stirred, and the light brown solid which formed was filtered. The solid was washed with water, dissolved in chloroform (200 mL), washed with saturated $NaHCO_3$, water, and dried over Na_2SO_4. The solution was passed through a bed of silica gel and on evaporation of the solvent yielded 5.7 g (75%) white crystalline solid, mp 118–119 °C. ^{1}H NMR (DMSO-d_6) 7.98 (m, 2H), 7.79 (d, 2H, J=8), 7.47 (d, 2H, J=8.0), 7.37 (m, 2H), 7.14 (s, 2H). ^{13}C NMR (DMSO-d_6) 151.3, 131.8, 130.6, 129.9, 125.7, 122.3, 122.0, 109.3. MS *m*/*e* 378 (M^+). The 2,5-bis(3-bromophenyl)furan thus obtained was used directly, without further characterization, in the next step.

A mixture of 2,5-bis(3-bromophenyl)furan (5.0 g, 13 mmol) and CuCN (4.15 g, 46 mmol) in 10 mL dry *N*-methyl-2-pyrrolidone was allowed to reflux under N_2 for 2 h (reaction progress followed by TLC, silica gel, Kodak plate, $CHCl_3$). The mixture was cooled, stirred with 150 mL of 10% aqueous NaCN for 5 h, filtered, washed with water and dried. The solid was dissolved in warm chloroform and passed through a neutral Al_2O_3 column and on evaporation of the solvent yielded 2,5-bis(3-cyanophenyl)furan as white crystalline needles 2.65 g (75.5%), mp 164–165 °C. ^{1}H NMR (DMSO-d_6) 8.32 (s, 2H), 8.14 (d, 2H, J=8), 7.72 (d, 2H, J=7.6), 7.63 (d, 1H, J=8), 7.61 (d, 1H, J=7.6). ^{13}C NMR (DMSO-d_6) 151.2, 130.7, 130.6, 129.8, 127.7, 126.8, 118.2, 112.1, 109.9. MS *m*/*e* 270 (M^+). Anal. calcd for: $C_{18}H_{10}N_2O$ C, 79.98; H, 3.73; N, 10.36. Found: C, 79.45; H, 3.81; N, 10.40. Alternatively, 2,5-bis(3-cyanophenyl)furan was prepared by cylodehydration of 1,4-di(3-cyanophenyl)butanedione, mp 201–202 °C, ^{1}H NMR (DMSO-d_6) 8.38 (s, 2H), 8.27 (d, 2H, J=7.6), 8.05 (d, 2H, J=7.6), 7.74 (m, 2H), 3.47 (s, 4H). ^{13}C NMR (DMSO-d_6) 197.2, 137.3, 135.9, 131.9, 131.3, 129.9, 127.7, 117.7, 111.9, 32.5. MS *m*/*e* 288 (M^+) obtained from 3-cyanobenzaldehyde using Stetter methodology (cf. ref 7).

A mixture of 2,5-bis(3-cyanophenyl)furan (2.5 g, 9.2 mmol) in 35 mL dry ethanol was saturated while stirring and cooling (0–5 °C) with dry HCl gas. The mixture was stirred at room temperature for 6 days (aliquots of the mixture were monitored by IR for the disappearance of the nitrile function), diluted with 75 mL dry ether and the resultant solid was filtered under nitrogen, washed with ether to yield the imidate ester hydrochloride 3.72 g (92%) after drying under vacuum at 30 °C for 5 h. A mixture of imidate ester HCl (0.87 g, 2 mmol) and dry ethylenediamine (0.13 g, 2.2 mmol) in 15 mL absolute ethanol was heated at reflux for 12 h. The solvent was removed under vacuum and the residue was treated with water and basified with 2 M NaOH. The precipitated solid was filtered, washed with water, dried and crystallized from chloroform/ether, to yield an off-white solid 0.57 g (80%) mp 222–224 °C. The free base (0.45 g, 1.3 mmol) was converted into the salt with ethanolic HCl to yield 0.51 g (88%) of a solid, mp 258–260 °C dec. ^{1}H NMR (DMSO-d_6) 8.65 (s, 2H), 8.16 (d, 2H, J=8), 7.91 (d, 2H, J=8), 7.67 (m, 2H), 7.22 (s, 2H), 4.03 (s, 8H). ^{13}C NMR (DMSO-d_6) 164.5, 151.9, 130.8, 129.9, 129.4, 127.4, 123.6, 122.8, 110.1, 44.4. MS (FAB) *m*/*e* 357 (M^++1). Anal. calcd. for: $C_{22}H_{20}N_4O$·2HCl·H_2O. C, 59.06; H, 5.40; N, 12.52. Found: C, 59.29; H, 5.07; N, 12.54.

2,5-Bis[3-(*N*-(3-dimethylaminopropyl)amidino)]phenylfuran tetrahydrochloride DB355. 2,5-Di(3-cyanophenyl)furan, from above, was converted into its imidate ester, subsequently allowed to react with 3-*N*,*N*-dimethyaminopropylamine, and finally converted into the hydrochloride salt using our standard procedure described for DB302 to yield an of hygroscopic off-white solid which was dried in vacuum at 70 °C for 24 h; mp 190–191 °C dec. ^{1}H NMR (DMSO-d_6) 8.25 (b, s, 2H), 8.13 (d, 2H, J=7.6), 7.73–7.63 (m, 4H), 7.23 (s, 2H), 3.56 (t, 4H, J=7.6), 3.21 (t, 4H, J=7.6), 2.79 (s, 12H), 2.12 (m, 4H). ^{13}C NMR (DMSO-d_6) 163.1, 152.2, 130.7, 129.9, 129.6, 128.3, 127.3, 123.4, 110.2, 54.4, 42.6, 40.1, 22.6. MS *m*/*e* 475 (M^++1). Anal. calcd for: $C_{28}H_{38}N_6O$·4HCl C, 52.66; H, 6.94; N, 13.16. Found: C, 52.63; H, 6.96; N, 13.10.

2,5-Bis[4{*N*-(4-dimethylaminobutyl)amidino}phenyl]furan tetrahydrochloride DB378. 2,5-Di(4-cyanophenyl)furan[37] was converted into its imidate ester, subsequently allowed to react with 4-dimethylaminobutylamine, and finally converted into the hydrochloride salt using our standard procedure described for DB302 to yield a yellow solid (86%); mp 205–208 °C dec. ^{1}H NMR (DMSO-d_6) 8.0 (d, 4H, J=7.6), 7.82 (d, 4H, J=7.6), 7.32 (s, 2H), 3.44 (t, 4H, J=6.4), 3.08 (t, 4H, J=7.2), 2.75 (s, 12H), 1.82–1.62 (m, 8H). ^{13}C NMR (DMSO-d_6) 162.9, 152.9, 134.4, 129.6, 127.8, 124.4, 112.0, 56.7, 42.7, 42.5, 24.7, 21.7. MS (FAB) *m*/*e* 503 (M^++1). Anal. calcd for: $C_{30}H_{42}N_6O$·4HCl·0.75 H_2O. C, 54.42; H, 7.23; N, 12.69. Found: C, 54.46; H, 7.06; N, 12.46.

2,5-Bis[4-[*N*-(6-dimethylaminohexyl)amidino]phenyl]furan tetrahydrochloride DB379. 2,5-Di(4-cyanophenyl)furan[37] was converted into its imidate ester, subsequently allowed to react with 6-dimethylaminohexylamine, and finally converted into the hydrochloride salt using our

standard procedure described for DB302 to yield a yellow solid (86%); mp 195–200 °C dec. ^{1}H NMR (DMSO-d_6) 8.0 (d, 4H, $J=8$), 7.84 (d, 4H, $J=8$), 7.31 (s, 2H), 3.43 (t, 4H, $J=6.4$), 3.02 (t, 4H, $J=8$), 2.72 (s, 12H), 1.72–1.61 (m, 8H), 1.44–1.32 (m, 8H). ^{13}C NMR (DMSO-d_6) 162.4, 152.6, 134.1, 129.2, 127.5, 124.1, 111.6, 56.8, 42.8, 42.3, 27.1, 25.7, 25.6, 23.7. MS (FAB) m/e 559 ($M^+ + 1$). Anal. calcd for: $C_{34}H_{50}N_6O$•4HCl•0.75H_2O. C, 56.87; H, 7.79, N, 11.70. Found: C, 56.88; H, 7.61; N, 11.63.

2,5-Bis[4-[*N*-(3-(*N*-pyrrolidinopropyl)amidino]phenyl]furan tetrahydrochloride DB380. 2,5-Di(4-cyanophenyl)furan[37] was converted into its imidate ester, subsequently allowed to react with 3-(*N*-pyrrolidino)propylamine, and finally converted into the hydrochloride salt using our standard procedure described for DB302 to yield a yellow solid (85%); mp 200–204 °C dec. ^{1}H NMR (DMSO-d_6) 7.99 (d, 4H, $J=8$), 7.31 (s, 2H), 7.90 (d, 4H, $J=8$), 7.31 (s, 2H), 3.60 (t, 4H, $J=6.4$), 3.28 (t, 4H, $J=7.2$), 3.05 (b, m, 4H), 2.52–2.46 (m, 4H), 2.18–2.10 (m, 4H), 2.06–1.96 (m, 4H), 1.94–1.86 (m, 4H). ^{13}C NMR (DMSO-d_6) 162.5, 152.5, 134.0, 129.1, 127.2, 123.8, 111.4, 53.2, 51.4, 23.9, 22.8. MS (FAB) m/e 526 ($M^+ + 1$). Anal. calcd for: $C_{32}H_{42}N_6O$•4HCl•1.5H_2O. C, 54.93; H, 7.05; N, 12.01. Found: C, 55.03; H, 7.02; N, 11.93.

2,5-Bis[3-([3-*N*,*N*-dimethylaminopropyl]amidino)phenyl]-pyrrole dihydrochloride DB381. A mixture of 1,4-di(3-bromophenyl)butanedione (3.96 g, 1 mmol) (see DB355) and anhydrous ammonium acetate (7.7 g, 0.1 mol) in 20 mL glacial acetic acid was heated at reflux, under nitrogen, for 5 h. The mixture was cooled and the solid which formed was filtered, washed with hexane and dried under vacuum at 60 °C for 24 h. The compound was recrystallized from $CHCl_3$/hexane to yield 2.98 g (79%), mp 143–145. ^{1}H NMR (DMSO-d_6/50 °C) 11.33 (s, 1H), 8.02 (s, 2H), 7.73 (d, 2H, $J=7.6$), 7.38–7.27 (m, 4H), 6.68(s, 2H). ^{13}C NMR (DMSO-d_6/50 °C) 134.4, 131.8, 130.3, 128.1, 125.9, 122.8, 122.0, 108.7. MS m/e 377 (M^+). 2,5-di(3-Bromophenyl)pyrrole (2.9 g, 7.7 mmol) was used directly without further characterization by heating with CuCN in *N*-methyl pyrrolidone in a standard procedure[1] to yield 2,5-di(3-cyanophenyl) pyrrole; 1.42 g (68%) of an off-white solid mp 210–212 °C. ^{1}H NMR (DMSO-d_6/50 °C) 11.44 (s, 1H), 8.24 (s, 2H), 8.06 (d, 2H, $J=8$), 7.61 (d, 2H, $J=8$), 7.56 (m, 2H), 6.80 (s, 2H). ^{13}C NMR (DMSO-d_6/50 °C) 133.1, 131.7, 129.6, 128.9, 128.2, 126.8, 118.6, 111.7., 109.4. Anal. calcd for: $C_{18}H_{11}N_3$: C, 80.29; H, 4.12; N, 15.60. Found: C, 80.29; H, 4.19; N, 15.51. The bis-nitrile was converted into its imidate ester, subsequently allowed to react with 3-*N*,*N*-dimethylaminopropylamine, and finally converted into the hydrochloride salt using our standard procedure to yield a brownish-yellow solid (92% yield); mp 197–199 °C dec. ^{1}H NMR (DMSO-d_6/D_2O) 8.22 (s, 2H), 8.10–8.0 (m, 2H), 7.62–7.51 (m, 4H), 6.75(s, 2H), 3.58–3.50 (b, m, 4H), 3.24–3.18 (b, m, 4H), 2.79 (s, 12H), 2.18–2.04 (m, 4H). ^{13}C NMR (DMSO-d_6/D_2O/50 °C) 163.9, 133.6, 132.9, 130.3, 129.5, 129.4, 125.8, 123.9, 109.8, 54.9, 45.1,40.4,23.0. MS (FAB) m/e 474 ($M^+ + 1$). Anal. calcd for: $C_{28}H_{39}N_7$•4HCl•2.5H_2O: C, 50.60; H, 7.28; N, 14.75. Found: C,50.61; H, 7.31; N, 14.72.

2,5-Bis[3(2-imidazolinyl)phenyl]pyrrole dihydrochloride DB382. 2,5-Di(3-cyanophenyl)pyrrole was converted into its imidate ester, subsequently allowed to react with ethylenediamine, and finally converted into the hydrochloride salt using our standard procedure (81% yield); mp 364–365 °C dec. ^{1}H NMR (DMSO-d_6/D_2O/50 °C) 8.54 (s, 2H), 8.13 (d, 2H, $J=8$), 7.72 (d, 2H, $J=7.6$), 7.58 (d, 2H, $J=8$). 7.57 (d, 2H, 7.6), 6.78 (s, 2H), 4.0 (s, 8H). ^{13}C NMR (DMSO-d_6/D_2O/50 °C) 165.3, 133.2, 132.4, 130.1, 129.8, 125.8, 124.3, 122.6, 109.6, 44.6. MS (FAB) m/e 356($M^+ + 1$). Anal. calcd for: $C_{22}H_{21}N_5$•2HCl•0.5H_2O: C, 60.41; H, 5.64; N, 16.01. Found: C, 60.58; H, 5.50; N, 16.07.

2,5-Bis[3-([3-*N*,*N*-dimethylaminoethyl]amidino)phenyl]-pyrrole dihydrochloride DB383. 2,5-Di(3-cyanophenyl) pyrrole was converted into its imidate ester, subsequently allowed to react with 2-*N*,*N*-dimethylaminoethylamine, and finally converted into the hydrochloride salt using our standard procedure to yield a brownish-yellow solid (90% yield); mp 297–299°C dec. ^{1}H NMR (DMSO-d_6/D_2O) 8.39 (s, 2H), 8.10 (d, 2H, $J=7.2$), 7.63 (d, 2H, $J=7.2$), 7.57 (d, 2H, $J=7.2$), 7.55 (d, 2H, $J=7.2$), 6.78 (s, 2H), 3.52 (b m, 4H), 2.89 (s, 12H), 2.18–2.04 (m, 4H). ^{13}C NMR (DMSO-d_6/D_2O/50 °C) 164.0, 133.2, 132.7, 129.9, 129.3, 129.1, 125.8, 124.1, 109.6, 54.4, 43.2,38.3. MS (FAB) m/e 446($M^+ + 1$). Anal. calcd for: $C_{26}H_{35}N_7$•4HCl: C, 52.80; H, 6.64; N, 16.58. Found: C, 52.63; H, 6.70; N, 16.43.

2,5-Bis[4-(*N*-(3-(4-*N*-methylpiperazino)propyl)amidino]-phenyl]furan hexahydrochloride DB394. 2,5-Di(4-cyanophenyl)furan[37] was converted into its imidate ester, subsequently allowed to react with 3-(*N*-methylpiperazino)propylamine, and finally converted into the hydrochloride salt using our standard procedure described for DB302 to yield a yellow solid (82%); mp 240–245 °C dec. ^{1}H NMR (DMSO-d_6/D_2O) 8.01 (d, 4H, $J=8$), 7.88 (d, 4H, $J=8$), 7.31 (s, 2H), 3.66 (b, 16H), 3.29 (t, 4H, $J=8$), 2.86 (s, 6H), 2.48 (b, 4H), 2.19–2.10 (m, 4H). ^{13}C NMR (DMSO-d_6) 162.7, 152.6, 134.1, 129.2, 127.3, 123.9, 111.5, 53.1, 49.6, 48.0, 47.8, 42.1, 22.3. MS (FAB) m/e 585 ($M^+ + 1$). Anal. calcd for: $C_{34}H_{48}N_8O$•6HCl•1.25H_2O C, 49.43; H, 6.89; N, 13.56. Found: C, 49.33; H, 6.91; N, 13.45.

2,5-Bis-4{*N*-(4-dimethylaminopropyl)amidino}phenyl-3-methylfuran tetrahydrochloride DB400. 2,5-di(4-cyanophenyl)-3-methylfuran[36] was converted into its imidate ester, subsequently allowed to react with 3-*N*,*N*-dimethylaminopropylamine, and finally converted into the hydrochloride salt using our standard procedure to yield a yellow solid (75% yield); mp 215–217 °C dec. ^{1}H NMR (DMSO-d_6/D_2O) 7.96 (d, 2H, $J=8.4$), 7.92 (d, 2H, $J=8.8$), 7.87 (d, 2H, $J=8.8$), 7.84 (d, 2H, $J=8.4$), 7.21 (s, 1H, $J=8.4$), 3.54–3.48 (m, 4H), 3.21–3.15 (m, 4H), 2.78 (s, 6H), 2.77 (s, 6H), 2.35 (s, 3H), 2.13–1.89 (m, 4H). ^{13}C NMR (DMSO-d_6/D_2O) 163.4, 151.2, 147.9, 135.2, 134.5, 133.8, 129.5, 129.3, 127.6, 127.0, 125.5, 124.4, 123.2 115.2, 54.9, 43.0, 40.4, 22.9, 12.3. MS m/e 489 (M^+). Anal. calcd for: $C_{29}H_{40}N_6O$•4HCl•1H_2O C, 53.37; H, 7.10; N, 12.88. Found: C, 53.54; H, 7.12; N, 12.83.

2,5-Bis{4-[*N*-(3-*N*,*N*-dimethyaminopropyl)amidino]phenyl}-3-(*p*-tolyloxy) furan tetrahydrochloride DB 414. 2,5-di(4-cyanophenyl)-3-tolyloxyfuran[38] was converted into its imidate ester, subsequently allowed to react with 3-*N*,*N*-dimethyaminopropylamine, and finally converted into the hydrochloride salt using our standard procedure to yield a yellow solid (90% yield); mp 205–206 °C dec. ^{1}H NMR (DMSO-d_6/D_2O) 7.99 (d, 2H, J=8.4), 7.97 (d, 2H, J=8.4), 7.80 (d, 4H, J=8.4), 7.19 (d, 2H, J=8.4), 7.12 (s, 2H), 7.03 (d, 2H, J=8.4), 3.52–3.46 (m, 4H), 3.18–3.14 (m, 4H), 2.78 (d, 6H, J=6.4), 2.77 (d, 6H, J=6.4), 2.24 (s, 3H), 2.11–2.08 (m, 4H). ^{13}C NMR (DMSO-d_6/D_2O) 163.6, 154.7, 151.1, 145.2, 139.6, 134.2, 134.0, 133.8, 131.1, 129.5, 128.4, 127.2, 124.7, 124.0, 117.5, 106.0, 55.0, 43.2, 40.4, 23.0, 20.6. MS *m*/*e* 581 (M^+). Anal. calcd for: $C_{35}H_{44}N_6O_2$·4HCl·1.5H_2O C, 55.78 ; H, 6.82; N, 11.15. Found: C, 55.93; H, 6.84; N, 11.05.

2,5-Bis[3-([3-*N*-methyl-*N*-(3-aminopropyl)aminopropyl] amidino)phenyl] furan hexahydrochloride DB420. 2,5-Di(3-cyanophenyl)furan from above, was converted into its imidate ester, subsequently allowed to react with 3,3′-diamino-*N*-methyldipropylamine, and finally converted into the hydrochloride salt using our standard procedure described for DB302 to yield (72%) of a very hygroscopic white solid which was dried in vacuum at 70 °C for 24 h; mp 250–253 °C dec. ^{13}C NMR (DMSO-d_6)/D_2O) 163.1, 152.3, 130.8, 129.9, 129.6, 128.4, 127.4, 123.6, 110.2, 53.1, 52.7, 40.3, 36.2, 22.4, 21.8. MS (FAB) *m*/*e* 561 (M^++1). Anal. calcd for: $C_{32}H_{48}N_8O$·6HCl·3H_2O C, 46.10; H, 7.25; N, 13.44. Found: C, 46.21; H, 7.51; N, 13.66.

2,5-Bis-3-[(*N*-(4-*N*,*N*-dimethylaminobutyl)amidino)]phenyl-furan tetrahydrochloride DB434. 2,5-di(3-cyanophenyl) furan (see above) was converted into its imidate ester, subsequently allowed to react with 4-*N*,*N*-dimethylaminobutylamine, and finally converted into the hydrochloride salt using our standard procedure to yield a very hygroscopic pale yellow solid (71% yield); mp 175–177 °C dec. ^{1}H NMR (DMSO/D_2O) 8.19–8.12 (m, 4H), 7.68–7.63 (m, 4H), 7.23 (s, 2H), 3.47 (t, 4H, J=6.8), 3.09 (m, 4H), 2.75 (s, 12H), 1.82–1.67 (m, 8H). ^{13}C NMR (DMSO-d_6) 163.6, 152.6, 131.1, 130.4, 130.1, 128.6, 127.5, 123.6, 110.5, 56.9, 42.7, 42.6, 24.7, 21.7. MS (FAB) *m*/*e* 503 (M^++1). Anal. calcd for: $C_{30}H_{42}N_6O$·4HCl·2H_2O C, 52.63; H, 7.36; N, 12.27. Found: C, 52.48; H, 6.92; N, 11.83.

2,4-Bis-4-(*N*-(3-dimethylaminopropyl)amidino)phenylpyrimidine pentahydrochloride DB436. 2,4-di(4-cyanophenyl) pyrimidine[39] was converted into its imidate ester, subsequently allowed to react with 4-dimethylaminopropylamine, and finally converted into the hydrochloride salt using our standard procedure described for DB302 to yield a very hygroscopic white solid (69%); mp 105–109 °C dec. ^{1}H NMR (DMSO/D_2O) 9.05 (d, 1H, J=5.2), 8.61 (d, 2H, J=8), 8.48 (d, 2H, J=8), 8.17 (d, 1H, J=5.2), 8.10 (d, 2H, J=8), 8.07 (d, 2H, J=8), 3.60 (t, 4H, J=7.2), 3.25–3.19 (m, 4H), 2.79 (s, 12H), 2.18–2.15 (m, 4H). ^{13}C NMR (DMSO/D_2O) 163.2, 163.1, 162.7, 162.3, 141.7, 140.7, 129.3, 129.0, 128.5, 127.9, 116.9, 54.5, 42.7, 40.2, 22.7. MS *m*/*e* (FAB) 487 (M^++1). Anal. calcd for: $C_{28}H_{38}N_8$·5HCl·2H_2O C, 47.70; H, 6.72; N, 15.89. Found: C, 47.99; H, 6.59; N, 15.67.

2,5-Bis-4-(*N*-(3-dimethylaminopropyl)amidino)phenyloxazole tetrahydrochloride DB449. 2,5-di(4-cyanophenyl) oxazole[40] was converted into its imidate ester, subsequently allowed to react with 4-dimethylaminopropylamine, and finally converted into the hydrochloride salt using our standard procedure described for DB302 to yield a pale yellow solid 85%, mp 205–208 °C dec. ^{1}H NMR (DMSO-d_6/D_2O) 8.28 (d, 2H, J=8.4), 8.05 (d, 2H, J=8.4), 8.06 (s, 1H), 7.95 (d, 2H, J=8.4), 7.91 (d, 2H, J=8.4), 3.55–3.48 (m, 4H), 3.25–3.15 (m, 4H), 2.79 (s, 12H), 2.16–2.04 (m, 4H). ^{13}C NMR (DMSO-d_6/D_2O) 162.8, 160.2, 150.6, 143.4, 131.6, 130.6, 129.4, 129.37, 128.5, 127.1, 126.7, 124.7, 54.4, 42.5, 40.2, 22.6. MS (FAB) *m*/*e* 476 (M^++1). Anal. calcd for: $C_{22}H_{37}N_7O$·4HCl·H_2O C, 50.70; H, 6.77; N, 15.33. Found: C, 50.46; H, 6.76; N, 15.07.

2,5-Bis-3-[(*N*-(4-*N*,*N*-dimethylaminohexyl)amidino)]phenyl-thiophene tetrahydrochloride DB492. 1,4-Bis-(3-bromophenyl)butanedione, from above, (3.96, 0.01 mol) and Lawesson's reagent (5 mmol, 2.02 g) in dry benzene was heated at reflux for 6 h (TLC monitored). The solvent was distilled under reduced pressure. The residue was dissolved in $CHCl_3$ and passed through a silica column using ether/hexane mixture to yield an off white solid 2.5 g (65%) mp 135–136 °C. ^{1}H NMR ($CDCl_3$) 7.75 (m, 2H), 7.51 (m, 2H), 7.40 (m, 2H), 7.26 (s, 2H), 7.23 (m, 2H). ^{13}C NMR ($CDCl_3$) 142.7, 136.2, 130.6, 130.4, 128.6, 124.9, 124.3, 123.1. MS *m*/*e* 394 (M^+). The 2,5-bis (3-bromophenyl) thiophene was used directly without further characterization to prepare 2,5-bis-(3-cyanophenyl) thiophene (60% yield, mp 178–180 °C) by the action of CuCN in *N*-methylpyrrolidone in a standard procedure.[36] ^{1}H NMR ($CDCl_3$) 7.87 (m, 2H), 7.82 (m, 2H), 7.57 (m, 2H,), 7.50 (m, 2H), 7.35 (s, 2H). ^{13}C NMR ($CDCl_3$) 142.3, 136.1, 131.0,. 129.9, 129.7, 129.0, 125.6, 118.3, 113.5. MS *m*/*e* 276 (M^+). 2,5-Di-(3-cyanophenyl) thiophene, without further characterization, was converted into its imidate ester, subsequently allowed to react with 4-dimethylaminohexyllamine, and finally converted into the hydrochloride salt using our standard procedure described for DB302 to yield (85%) a very hygroscopic solid; mp 147–150 °C dec. ^{1}H NMR (DMSO-d_6/D_2O) 8.11 (b, 2H), 7.95 (d, 2H, J=8), 7.75 (s, 2H), 7.73 (d, 2H, J=8), 7.64 (t, 2H, J=8), 3.49 (t, 4H, J=7.2), 3.02 (t, 4H, J=7.2), 2.72 (s, 12H), 1.73–1.65 (m, 8H), 1.43–1.35 (m, 8H). ^{13}C NMR (DMSO-d_6/D_2O) 162.3, 141.9, 133.9, 129.7, 129.6, 129.5, 127.2, 126.5, 124.9, 56.5, 42.5, 41.9, 26.8, 25.4, 25.3, 23.2. MS (FAB) *m*/*e* 575 (M^++1). Anal. calcd for: $C_{34}H_{50}N_6S$·4HCl·H_2O C, 55.43; H, 7.39; N, 111.40. Found: C, 55.41; H, 7.71; N, 11.40.

2,5-Bis-3-[(*N*-(4-*N*,*N*-dimethylaminobutyl)amidino)]phenyl-thiophene tetrahydrochloride DB493. 2,5-Di(3-cyanophenyl)thiophene was converted into its imidate ester, subsequently allowed to react with 4-dimethylaminobutylamine, and finally converted into the hydrochloride salt using our standard procedure described for DB302

to yield (90%) a pale yellow hygroscopic solid (90%); mp 170–172 °C dec. ^{1}H NMR (DMSO-d_6/D_2O) 8.08 (b, 2H), 7.96 (d, 2H, J = 7.6), 7.72 (d, 2H, J = 7.6), 7.71 (s, 2H), 7.63 (t, 2H, J = 7.6), 3.52 (t, 4H, J = 6.8), 3.10 (t, 4H, J = 7.2), 2.75 (s, 12H), 1.84–1.72 (m, 8H). ^{13}C NMR (DMSO-d_6/D_2O) 162.7, 142.1, 134.1, 129.9, 129.8, 129.7, 127.3, 126.6, 124.9, 56.3, 42.3, 42.1, 24.4, 21.2. MS (FAB) 519 ($M^+ + 1$). Anal. calcd for: $C_{30}H_{42}N_6S \cdot 4HCl \cdot 0.75H_2O$ (676.11). C, 53.29; H, 6.78; N, 12.43. Found: C, 53.26; H, 7.00; N, 12.25.

2,5-Bis-4-(*N*-(3-dimethylaminopropyl)amidino)phenylpyrrole tetrahydrochloride DB522. 2,5-di(4-cyanophenyl)pyrrole (**32**) was converted into its imidate ester, subsequently allowed to react with 4-dimethylaminopropylamine, and finally converted into the hydrochloride salt using our standard procedure described for DB302 to yield a yellow solid (88%); mp 273–275 °C dec. ^{1}H NMR (DMSO-d_6/D_2O) 7.99 (d, 4H, J = 8.4), 7.79 (d, 4H, J = 8.4), 6.86 (s, 2H), 3.57–3.52 (m, 4H), 3.22–3.16 (m, 4H), 2.79 (s, 12H), 2.14–2.05 (m, 4H). ^{13}C NMR (DMSO-d_6/D_2O) 162.7, 152.6, 134.1, 129.2, 127.3, 123.9, 111.5, 53.1, 49.6, 42.1, 22.3. MS (FAB) m/e 474 ($M^+ + 1$). Anal. calcd for: $C_{28}H_{39}N_7 \cdot 4HCl \cdot 2H_2O$ C, 51.30; H, 7.22; N, 14.96. Found: C, 51.19; H, 7.41; N, 14.79.

RNA and peptides. The RRE hairpin and RRE and TAR duplex strands (Fig. 1(a)) were purchased from Cruachem with HPLC purification. Oligonucleotide concentrations were determined by absorbance at 260 nm. Single-strands of RNAs were end-labeled using [γ-^{32}P]ATP and T4 polynucleotide kinase under standard conditions.[33] For efficient labeling, it is very important that the RNA is free of any impurities that would be preferentially labeled. The HPLC purified RRE hairpin was labeled very poorly and for this reason the RRE hairpin was purified by electrophoresis through a denaturing gel (20% acrylamide, 50% urea). Individual bands detected by UV shadowing were excised, eluted and Centriconed to remove ions. After radiolabeled as previous described,[33] the sample was suspended in denaturing loading buffer and purified on a 20% denaturing polyacrylamide gel. After autoradiography, the band corresponding to the 30 mer RRE hairpin was excised from the gel and eluted in 500 μL elution buffer (0.5 M NH_4OAc, 10 mM $Mg(OAc)_2$, 1.0 mM EDTA and 0.1% SDS) at 0 °C overnight. The RRE oligomer was precipitated from the supernatant by addition of 80% cold ethanol and was centrifuged for 30 min. The resulting pellet was washed twice with cold 80% ethanol. The concentrations of labeled RNA were calculated from the specific activity of ^{32}P incorporation. The concentrations of unlabeled RNA solutions were quantitated by spectrophotometry. The RRE hairpin model stock solutions were prepared by heating the unlabeled or ^{32}P-5′-end labeled RNA strand at micromolar concentrations to 90 °C for 2 min in sodium phosphate buffer (10 mM phosphate, 1 mM EDTA, 0.1 M NaCl, adjusted to pH 7.0 with NaOH) with slow cooling to room temperature. The duplex model stock solutions were prepared by heating the mixtures of ^{32}P-5′-end labeled complementary strands at micromolar concentrations to 90 °C for 2 min in the same buffer with slow cooling to room temperature. For all studies, the RNA hairpin and duplexes were reannealed by heating to 90 °C and cooled down in room temperature prior to use.

The Rev-17 peptide (Fig. 1(a)) with the sequence defined by Tan et al.[30] was purchased from Chiron. The peptide is succinylated at the amino termini and amidated at the carboxy termini, modifications that have been shown to increase alpha-helicity of the peptide and its binding to RRE.[30] The Tat-24 peptide (Fig. 1(a)) with the sequence defined by Long et al.[34] was prepared as previous described.[33]

Thermal denaturation experiments

The RRE duplex melting studies were conducted in Rev dilution buffer (10 mM phosphate, 1 mM EDTA, 0.1 M NaCl, 1 mM MgCl, 1 mM DTT). The thermal dissociation studies were performed with a Cary 3 spectrophotometer by following the absorbance change at 260 nm as a function of temperature. The temperature was controlled by Varian software with a Cary temperature controller that was programmed to raise the temperature at a rate at 0.5 °C/min. A thermister fixed into a reference cuvette was used to monitor the temperature. T_m values were determined from the first derivative plots.[41] Compounds are compared by the increase in T_m ($\Delta T_m = T_m$ of complexes$- T_m$ of free nucleic acids) that they produce at each concentration.

Gel shift assay for RRE/Rev and TAR/Tat complexes. RNA ^{32}P-labeled duplexes were formed as described above, and the stock solution was diluted and added to a sodium phosphate buffer. RNA solutions were aliquoted (8 μL), and increasing concentrations of Rev-17 peptide or Tat-24 peptide were added (2 μL) to achieve final peptide concentration ranges. The final duplex concentration was 5 nM. The final reaction conditions in a 12 μL total volume were 10 mM phosphate, 1 mM EDTA, 0.1 M NaCl, 1 mM $MgCl_2$, 1 mM DTT, 25 mg/mL yeast tRNA (Sigma), and 10% glycerol. The reaction mixtures were incubated for at least 15 min, and samples (3 μL) were then applied to a 12% native polyacrylamide gel (20×20 cm) cast in 1×TBE (90 mM Tris/borate and 2 mM EDTA at pH 7.7) and prequilibrated overnight at 20 °C. The samples were electrophoresed for 4 h at 220 V at 20 °C. The gels were fixed, dried in vacuo at 80 °C, and autoradiographed (Biomax, Kodak). Autoradiographs were scanned on a densitometer (PDI, Inc.) and quantitated using software supplied by PDI.

Competitive gel shift assay for inhibitors of RRE/Rev TAR/Tat complexation. As described above, labeled RRE duplex or hairpin solution (2 μL) was incubated with 6 μL binding reaction buffer (above). To this solution was added 2 μL of competitive inhibitor at a range of concentrations and either the Rev-17 or Tat-24 peptide solution (2 μL). Labeled RNA duplex and competitive inhibitor were pre-mixed in reaction buffer to prevent premature interaction with Rev peptide as described by Daly et al.[42] Incubation, electrophoresis and imaging were the same as described above. The IC_{50} was calculated by fitting the densitometer data to the following equation:

$$\% \text{ Inhibition} = \frac{[\text{drug}]}{[\text{drug}] + IC_{50}}$$

where % Inhibition is the percent of intensity of the free RNA band; [drug] is the compound concentration after each addition; IC_{50} is the calculated concentration of the compound when the intensity of the upper band is equal to the lower band.

Acknowledgements

This research was supported by National Institutes of Health Grants GM-54896 and GM-61587.

References

1. Tinoco, I. J.; Bustamanta, C. *J. Mol. Biol.* **1999**, *293*, 271.
2. Gesteland, R. F.; Atkins, J. F., Eds. *The RNA World II*; Cold Spring Harbor Laboratory: Plainview, NY, 1993; 1–630.
3. Niedle, S., Eds. *Oxford Handbook of Nucleic Acid Structure*; Oxford University Press, Oxford, 1999; p 608.
4. Draper, D. E. *J. Mol. Biol.* **1999**, *293*, 255.
5. Wong, C.-H.; Hendrix, M.; Manning, D. D.; Rosenbohm, C.; Greenberg, W. A. *J. Am. Chem. Soc.* **1998**, *120*, 8319.
6. Hendrix, M.; Priestley, E. S.; Joyce, G. F.; Wong, C.-H. *J. Am. Chem. Soc.* **1997**, *119*, 3641.
7. Sucheck, S. J.; Wong, A. L.; Koeller, K. M.; Boehr, D. D.; Draker, K.-A.; Sears, P.; Wright, G. J.; Wong, C.-H. *J. Am. Chem. Soc.* **2000**, *122*, 5230.
8. Sucheck, S. J.; Greenberg, W. A.; Tolbert, T. J.; Wong, C.-H. *Angew. Chem., Int. Ed.* **2000**, *39*, 1080.
9. Chow, C. S.; Bogdan, F. M. *Chem. Rev.* **1997**, *97*, 1489.
10. Pearson, N. D.; Prescott, C. D. *Chem. Biol.* **1997**, *4*, 409.
11. Hermann, T.; Westhof, E. *Curr. Opin. Biotech.* **1998**, *9*, 66.
12. Tor, Y. *Angew. Chem.* **1999**, *38*, 1579.
13. Hermann, T.; Westhof, E. *J. Med. Chem.* **1999**, *42*, 1250.
14. Wilson, W. D.; Li, K. *Curr. Med. Chem.* **2000**, *7*, 73.
15. Puglisi, E. V.; Puglisi, J. D. In *RNA Structure and Function*; Simons, R. W. Grunberg-Manago, M., Eds, Cold Spring Harbor Press, Cold Spring Harbor 1998, p 117.
16. Lynch, S. R.; Recht, M. I.; Puglisi, J. D. *Meth. Enz.* **1999**, *317*, 240.
17. Schroeder, R.; nov Ahsen, U. *Nucl. Acids Mol. Biol.* **1996**, *10*, 53.
18. Hermann, T.; Westhof, E. *J. Mol. Biol.* **1998**, *276*, 903.
19. Rogers, J.; Chang, A. H.; Ahsen, U. v.; Schroeder, R. *J. Mol. Biol.* **1996**, *36*, 916.
20. Ahsen, U. v.; Davies, J.; Schroeder, R. *Nature* **1991**, *353*, 368.
21. Mei, H.-Y.; Galan, A. A.; Halim, N. J.; Mack, D. P.; Moreland, J. W.; Sanders, K. B.; Truong, H. N.; Czarnik, A. J. *Bioorg. Med. Chem. Lett.* **1995**, *5*, 2755.
22. Wang, S.; Huber, P. W.; Cui, M.; Czarnik, A. W.; Mei, H.-Y. *Biochemistry* **1998**, *37*, 5549.
23. Zapp, M. L.; Stern, S.; Green, M. R. *Cell* **1993**, *74*, 969.
24. Rogers, M. J.; Bukhman, Y. V.; McCutchan, R. F.; Draper, D. E. *RNA* **1997**, *3*, 815.
25. Conn, G. L.; Gutell, R. R.; Draper, D. E. *Biochemistry* **1998**, *37*, 11980.
26. Ratmeyer, L.; Zapp, M. L.; Green, M. R.; Vinayak, R.; Kumar, A.; Boykin, D. W.; Wilson, W. D. *Biochemistry* **1996**, *35*, 13689.
27. Zapp, M. L.; Young, D. W.; Kumar, A.; Singh, R.; Boykin, D. W.; Wilson, W. D.; Green, M. R. *Bioorg. Med. Chem.* **1997**, *5*, 1149.
28. Li, K.; Xiao, G.; Rigl, T.; Kumar, A.; Boykin, D. W.; Wilson, W. D. In *Structure, Motion, Interaction and Expression of Biological Macromolecules*; Sarma, R. H., Sarma, M. H., Eds.; Adenine: 1998; 137–145.
29. Pritchard, C. E.; Grasby, J. A.; Hamy, F.; Zacharek, A. M.; Singh, M.; Karn, J.; Gait, M. J. *Nucl. Acids Res.* **1994**, *22*, 2592.
30. Tan, R.; Chen, L.; Buettner, D. H.; Frankel, A. D. *Cell* **1997**, *73*, 1031.
31. Peterson, R. D.; Bartel, D. P.; Szostak, J. W.; Horvath, S. J.; Feigon, J. *Biochemistry* **1994**, *33*, 5357.
32. Li, K.; Fernandex-Saiz, M.; Rigl, C. T.; Kumar, A.; Ragunathan, K. G.; McConnaughie, A. W.; Boykin, D. W.; Schneider, H.-J.; Wilson, W. D. *Bioorg. Med. Chem.* **1997**, *5*, 1157.
33. Rigl, C. T.; Lioyd, D. H.; Tsou, D. S.; Gryaznov, S. M.; Wilson, W. D. *Biochemistry* **1997**, *36*, 650.
34. Long, K. S.; Crothers, D. M. *Biochemistry* **1995**, *34*, 8885.
35. Luedtke, N. W.; Tor, Y. *Angew. Chem. Int. Ed.* **2000**, *39*, 1788.
36. Das, B. P.; Boykin, D. W. *J. Med. Chem.* **1977**, *20*, 1219.
37. Bajic, M.; Kumar, A.; Boykin, D. W. *Heterocyclic Comm.* **1996**, *2*, 135.
38. Kumar, A.; Boykin, W. D. *Syn. Commun.* **1995**, *25*, 2071.
39. Kumar, A.; Boykin, D. W.; Wilson, W. D. *Eur. J. Med. Chem.* **1996**, *31*, 767.
40. Das, B. P.; Wallace, R. A.; Boykin, D. W. *J. Med. Chem.* **1980**, *23*, 578.
41. Wilson, W. D.; Tanious, F. A.; Fernandez-Saiz, M.; Rigl, C. T. *Methods Mol. Med.* **1997**, *90*, 219.
42. Daly, T. J.; Doten, R. C.; Rennert, P.; Auer, M.; Jaksche, H.; Donner, A.; Fisk, G.; Rusche, J. R. *Biochemistry* **1993**, *32*, 10497.